

Disruption of Cellular Gene Expression on TGF- $\beta$  Signaling by Perfluorooctanoic Acid (PFOA) and its Novel Substitute Perfluoro(2-methyl-3-oxahexanoic) Acid (GenX) in Vitro

By

Hongran Ding

DKU Global Health Program  
Duke University

Defense Date: March 27, 2024

Approved:

Anastasia Tsigkou, Advisor

Chenkai Wu, Chair

Marius Wamsiedel

Thesis submitted in partial fulfillment of the requirements for the degree of Master of Science in the DKU Global Health Program in The Graduate School of Duke University  
2024

ABSTRACT

Disruption of Cellular Gene Expression on TGF- $\beta$  Signaling by Perfluorooctanoic Acid (PFOA) and its Novel Substitute Perfluoro(2-methyl-3-oxahexanoic) Acid (GenX) in Vitro

By

Hongran Ding

DKU Global Health Program  
Duke University

Defense Date: March 27, 2024

Approved:

Anastasia Tsigkou, Advisor

Chenkai Wu, Chair

Marius Wamsiedel

An abstract of a thesis submitted in partial fulfillment of the requirements for the degree of Master of Science in the DKU Global Health Program in The Graduate School of Duke University

2024

Copyright by  
Hongran Ding  
2024

## **Abstract**

**Introduction:** This study explores the cytotoxic effects of Per- and polyfluoroalkyl substances (PFAS), specifically focusing on Perfluorooctanoic acid (PFOA) and its industrial substitute, Gen-X, on a set of human cancer cell lines. PFAS are synthetic chemicals with widespread use and environmental persistence, raising concerns over their potential bio accumulative properties and toxicity. Research aims to elucidate the mechanistic impact of PFOA and Gen-X exposure on cell viability, gene expression, and protein signaling pathways including TGF- $\beta$ /SMAD, p53 signaling across melanoma (A375), renal (SN12C), liver (HepG2), and colon (SW620) cancer cells.

**Method:** Employing a comprehensive experimental approach, the study assessed cytotoxicity using the CCK-8 assay, protein expression via Western blot analyses, and gene expression changes through RT-PCR. Four human cancer cell lines were exposed to varying concentrations of PFOA and Gen-X to determine their semi-inhibitory concentrations (IC50) and to analyze the subsequent biological effects.

**Result:** The results highlighted distinct cytotoxic profiles for PFOA and Gen-X across the examined cell lines, revealing variations in cellular susceptibility and resistance. Melanoma cancer cells (A375) displayed high sensitivity to PFOA but greater tolerance to Gen-X, while renal cancer cells (SN12C) showed significant resistance to both compounds. Molecular analyses indicated that exposure to PFOA and Gen-X modulates

the TGF- $\beta$ /SMAD signaling pathway and activates DNA damage response markers. Furthermore, alterations in the expression of genes related to the cell cycle, apoptosis, and metabolic processes were observed, suggesting potential genotoxic and carcinogenic effects.

**Conclusion:** The study provides insights into the differential cytotoxic effects of PFOA and Gen-X on human cancer cell lines, underscoring the complex interaction between these PFAS and cellular mechanisms. The findings indicate that PFAS exposure can significantly impact cell viability, gene expression, and protein signaling pathways, contributing to our understanding of their toxicological profile. Given the environmental persistence and widespread use of PFAS, these results underscore the need for further research into their biological impacts and the development of targeted intervention strategies to mitigate their health risks.

# Contents

ABSTRACT .....	IV
LIST OF TABLES .....	VIII
LIST OF FIGURES .....	IX
CHAPTER 1 BACKGROUND AND INTRODUCTION .....	1
1.    BACKGROUND AND INTRODUCTION .....	1
1.1.    Introduction .....	1
1.2.    Perfluorooctanoic acid (PFOA) .....	2
1.2.1.    Pathways of human exposure to PFOA .....	2
1.2.2.    Toxicity of PFOA to human health .....	3
1.3.    Gen-X .....	4
1.4.    Cytotoxicity studies of PFOA and Gen-X .....	5
1.4.1.    Thyroid cells .....	5
1.4.2.    Hepatocarcinoma cell line .....	6
1.4.3.    Other cell lines .....	6
1.5.    Aim of present study .....	7
CHAPTER 2. MATERIALS AND METHODS .....	8
2.    MATERIALS AND METHODS .....	8
2.1.    Chemicals .....	8
2.2.    Cell culture maintenance .....	9
2.2.1.    Cell culturing .....	9
2.2.2.    Cell passaging .....	10
2.2.3.    Cell freezing .....	11
2.2.4.    Cell thawing .....	11
2.3.    Cell viability assay .....	12
2.3.1.    Cell plating .....	12
2.3.2.    Toxin exposure .....	13
2.3.3.    CCK-8 assay .....	13
2.4.    Western blot .....	13
2.4.1.    Protein extraction .....	14
2.4.2.    Sample preparation .....	14
2.4.3.    SDS-PAGE .....	15
2.4.4.    Membrane transferring .....	15
2.4.5.    Blocking .....	16
2.4.6.    Primary antibody incubation .....	16
2.4.7.    Secondary antibody incubation .....	16
2.4.8.    Protein Imaging .....	17

2.5.	<i>RNA extraction</i> .....	17
2.6.	<i>cDNA Synthesis</i> .....	18
2.7.	<i>RT-PCR</i> .....	18
2.8.	<i>Statistical analysis</i> .....	19
CHAPTER 3: RESULTS.....		20
3.	RESULTS .....	20
3.1.	<i>Cytotoxicity assessment</i> .....	20
3.1.1.	A375 cell line .....	20
3.1.2.	SN12C cell line .....	21
3.1.3.	SW620 cell line.....	21
3.1.4.	HepG2 cell line.....	21
3.2.	<i>Protein expression results</i> .....	23
3.2.1.	Abundance of $\gamma$ -H2A.X.....	24
3.2.2.	Pathway analysis of PFOA and Gen-X impact.....	25
3.2.3.	Expression from A375 cell line .....	26
3.2.4.	Expression from SN12C cell line .....	29
3.2.5.	Expression from HepG2 cell line .....	31
3.2.6.	Expression from SW620 cell line.....	34
CHAPTER 4: DISCUSSION AND CONCLUSION .....		37
4.	DISCUSSION AND CONCLUSION.....	37
4.1.	<i>Assessment of PFOA and Gen-X toxicity to cancer cells</i> .....	37
4.1.1.	Protein expression assessment.....	38
4.1.2.	PFOA and Gen-X induce significant changes in gene expression in four kinds of human cancer cell lines .....	39
4.1.2.1.	Response of the A375 cell line .....	40
4.1.2.2.	Response of the SN12C cell line.....	43
4.1.2.3.	Response of the HepG2 cell line .....	44
4.1.2.4.	Response of the SW620 cell line.....	46
4.1.3.	Strength and limitations.....	47
4.2.	<i>Conclusion</i> .....	49
Appendix A .....		51
Appendix B .....		53
Appendix C .....		55
Reference list.....		56

## List of Tables

Table 1: IC <sub>50</sub> (with 95% confidence intervals) of A375, SN12C, SW620, and HepG2 cells in response to PFOA and Gen-X, obtained by CCK-8 assay, were estimated by fitting the results using nonlinear regression. ....	22
---	----

## List of Figures

Figure 1: Viability of (A) A375, (B) SN12C, (C) SW620, (D) HepG2 cells exposed to PFOA by CCK-8 assay.....	22
Figure 2: Viability of (A) A375, (B) SN12C, (C) SW620, (D) HepG2 cells exposed to Gen-X by CCK-8 assay.....	23
Figure 3: Western blot analysis of abundance of $\gamma$ -H2A.X (15 kDa) in (a) A375, (b) SN12C, (c) HepG2, (d) SW620.....	24
Figure 4: Altered gene expression (left) and protein expression (right) in A375 cells following exposure to PFOA.....	28
Figure 5: Altered gene expression (left) and protein expression (right) in A375 cells following exposure to Gen-X.....	28
Figure 6: Altered gene expression (left) and protein expression (right) in SN12C cells following exposure to PFOA.....	30
Figure 7: Altered gene expression (left) and protein expression (right) in SN12C cells following exposure to Gen-X.....	31
Figure 8: Altered gene expression (left) and protein expression (right) in HepG2 cells following exposure to PFOA.....	33
Figure 9: Altered gene expression (left) and protein expression (right) in HepG2 cells following exposure to Gen-X.....	33
Figure 10: Altered gene expression (left) and protein expression (right) in SW620 cells following exposure to PFOA. ....	35
Figure 11: Altered gene expression (left) and protein expression (right) in SW620 cells following exposure to Gen-X.....	36

# Chapter 1 Background and Introduction

## 1. Background and Introduction

### 1.1. Introduction

Per - and polyfluoroalkyl substances (PFAS) are a series of synthetic organic fluorides with special physical and chemical properties that are resistant to dust, water and grease (Buck et al., 2011). As a consequence of the intrinsic chemical stability of PFAS, the molecular constituents of this group of synthetic chemicals display a remarkably slow rate of decomposition, leading to a persistent and pervasive presence of PFAS in various environmental media, such as water, soil, and air (Kwiatkowski et al., 2020).

The persistent accumulation of PFAS in the environment is significantly aggravated by the extensive and ubiquitous employment of these synthetic chemicals in a multitude of industrial and consumer applications (Evich et al., 2022). These include personal care products (PCPs), aqueous film-forming foams (AFFF), ski wax, cosmetics, food contact materials, textile treatments designed for stain and water repellency, medical devices, as well as the use of PFAS-based membranes in fuel cells and chloralkaline processes (De Silva et al., 2021). The resulting contamination of the environment with these compounds is a growing public health and environmental concern.

A vast amount of research has been conducted to explore the pathways of human exposure to PFAS, focusing on two of the most widely studied chemicals in this class, perfluorooctanoic acid (PFOA) and perfluorooctane sulfonic acid (PFOS). Moreover,

Gen-X, a substitute for PFOA, has been the focus of research in recent years.

## **1.2. Perfluorooctanoic acid (PFOA)**

### **1.2.1. Pathways of human exposure to PFOA**

The major routes of exposure to PFOA include dietary intake, inhalation of indoor air, dermal absorption, and inhalation of house dust. Dietary intake is the primary exposure route and usually accounts for the majority of total PFOA intake, which contributed 92% of the PFOA total intake of human bodies (Poothong et al., 2020). This is followed by inhalation of house dust, inhalation of indoor air, and dermal absorption; however, significant differences exist between individuals (Poothong et al., 2020). In addition, indirect exposure is also an important uptake route, especially inhalation of indoor air through the precursor substance of PFOA, and 8:2FTOH (2,2,4-trimethyl-1,3-pentenediol diisobutyrate), a chemical compound used in various products, including as a plasticizer in nail polish and other cosmetics. (Eriksson & Kärman, 2015).

As a result of multiple exposure pathways, studies have consistently demonstrated the widespread presence of PFOA in the blood and breast milk of individuals across various geographical regions, which highlights the pervasive nature of human exposure to these highly persistent and bio accumulative contaminants (Jian et al., 2018). Moreover, research has demonstrated the ubiquitous occurrence of PFOA in various human biomonitoring matrices, including but not limited to urine, serum, hair, and nails (B. Liu et al., 2020; Wang et al., 2018).

### **1.2.2.Toxicity of PFOA to human health**

A series of investigations have been dedicated to investigating the potential adverse effects of exposure to PFOA on human health. In epidemiologic studies, a positive association between PFOA and increased risk of kidney cancer has been reported (Shearer et al., 2021; Vieira et al., 2013). A study by Vieira et al. (2013) also found a positive correlation between PFOA and increased risk of testicular cancer. However, there are also studies that have concluded that there is no causal relationship between PFOA exposure and cancer. Some of these studies have concluded that there is currently no evidence that PFOA causes an increased overall cancer risk, while some have suggested that the association between PFOA and kidney and testicular cancer may be due to chance (Bartell & Vieira, 2021).

In terms of biology, many studies have identified the potential hazards of PFOA for humans. Firstly, PFOA exhibits immunotoxicity, potentially leading to a range of health impacts including the disruption of the immune system and its associated functions (Sunderland et al., 2019). Secondly, PFOA, also classified as an endocrine disrupting chemical (EDC), has been shown to have the ability to regulate a variety of endocrine functions that may lead to the development or promotion of cancer. Specifically, many studies have found that PFOA can promote the growth of prostate and breast cancer cells through different signaling pathways, suggesting that this compound may contribute to the development and progression of these diseases (Charazac et al., 2019, 2022). Finally, PFOA influences human metabolism. PFOA exposure has been found

to be associated with metabolic abnormalities, mainly in the form of dyslipidemia. Animal studies do suggest that animals exposed to PFOA may exhibit decreases in total cholesterol and triglyceride levels. In contrast, human epidemiologic studies observing populations in real-world settings typically report elevated serum cholesterol levels because of PFOA exposure. These differences between human and animal studies may be due to differences in metabolism, level of exposure, duration of exposure, or other environmental and genetic factors that may vary widely between humans and experimental animals (Ubel et al., 1980). In addition, human studies have shown an association between PFOA and metabolic abnormalities such as high cholesterol and hyperuricemia (Gilliland & Mandel, 1993). Studies have also found that exposure to PFOA in children leads to elevated serum cholesterol (Lin et al., 2013). However, the results of current studies on the effects of PFOA on human metabolism are inconsistent, and further in-depth studies are needed to clarify the mechanisms and the exact extent of the effects.

### **1.3. Gen-X**

Gen-X is a new generation of PFAS and is considered as an industrial substitute for PFOA. Gen-X belongs to a shorter chain of perfluorinated compounds and is considered a safer alternative because it has a shorter retention time in the environment compared to longer chain compounds such as PFOA (Zane & Schultz, 2020). It was found that Gen-X is highly migratory in the environment and can be detected far from its source

(Coperchini et al., 2020). Studies have shown that Gen-X is more toxic compared to PFOA and PFOS. Animal model studies have shown that Gen-X is both hepatotoxic and carcinogenic (Gomis et al., 2018; Sun et al., 2019). Gen-X can activate the peroxisome proliferator-activated receptor alpha (PPAR $\alpha$ ) pathway in mouse hepatocyte cell lines and cause cellular damage (Sun et al., 2019). Gen-X can also cause upregulation of 28 genes associated with the PPAR signaling pathway, which affect lipolysis, fatty acid uptake, and lipoprotein transport and assembly (Conley et al., 2019). These studies also found that Gen-X produced similar effects in the livers of pregnant mice (Blake et al., 2020).

#### **1.4. Cytotoxicity studies of PFOA and Gen-X**

##### **1.4.1. Thyroid cells**

PFOA has been proven to enter the thyroid gland and act as an endocrine thyroid disruptor, which in some cases can lead to the development of thyroid lesions and even cancer (Coperchini et al., 2017). Recent studies have shown that both PFOA and Gen-X have a negative effect on thyroid cells. It was demonstrated that both PFOA and Gen-X reduced the viability of thyroid cells (Zhang et al., 2021). The proliferation rate of cells exposed to PFOA and Gen-X was significantly reduced compared to cells not exposed to PFAS. This finding also suggests that, in addition to acute cytotoxicity to cells, PFOA and Gen-X have long-term adverse effects on the health of thyroid cells (Zhang et al., 2021). In addition, in the study by Zhang *et al.* (2021), Gen-X was found

to be more toxic than PFOA under the same conditions.

#### **1.4.2. Hepatocarcinoma cell line**

Previous animal studies have shown that PFOA accumulates in the liver of experimental animals and causes a range of liver lesions. Therefore, the liver is considered a target organ for PFOA accumulation and toxicity (Son et al., 2008). In a study by Abudayyak *et al.* (2021), it was found that PFOA at low concentrations caused cell death mainly through the apoptotic pathway, whereas high concentrations resulted in an increased proportion of necrotic cells. In addition, PFOA significantly altered the expression levels of intracellular substances, including interleukin-6 (IL-6) and interleukin-8 (IL-8), as well as glutathione (GSH) and catalase (CAT).

#### **1.4.3. Other cell lines**

Currently, the research concerning the toxicity of PFOA and its emerging alternative, Gen-X, on other cell lines remains limited. A notable study conducted by Pierozan *et al.* (2020) has specifically addressed the carcinogenic effects of PFOA on human breast epithelial cells. This study concluded that PFOA appears to have a promotional effect on the carcinogenesis of human breast epithelial cells, indicating a potential risk associated with exposure to this chemical. This finding is significant as it adds to the growing body of evidence on the harmful impacts of PFOA on human health, highlighting the need for further research in this area to understand the full extent of its

effects, as well as those of its alternatives like Gen-X, on different types of cells. However, more cell-based studies are still needed to investigate the potential effects of PFOA and Gen-X on cell proliferation, polarization, and gene expression.

### **1.5. Aim of present study**

The main objective of this research work is to study the cytotoxic effects of perfluorooctanoic acid (PFOA) and its emerging alternative Gen-X on human health. To this end, their potential effects on cell viability, altered protein expression and gene expression changes in various human cancer cell lines will be comprehensively investigated. Specifically, this study will focus on human hepatocellular carcinoma cell line (HepG2) representing the major organ that metabolizes toxic compounds; human kidney cancer cell line (SN12C) representing the kidneys where metabolic wastes are filtered; human colon cancer cell line (SW620) representing digestive system exposures; and human melanoma cell line (A375) representing skin contact exposures. By studying these different cell types, the study aims to gain a comprehensive understanding of the toxicological effects of PFOA and Gen-X, thereby revealing the wide-ranging effects of exposure to these chemicals. The results of this study could contribute further understanding of the molecular mechanisms underlying the effects of these substances and could raise health awareness of PFAS among regulators and the general public which will further inform regulatory decisions and public health policies regarding the use and handling of these substances.

## Chapter 2. Materials and methods

### 2. Materials and methods

#### 2.1. Chemicals

Perfluorooctanoic acid (PFOA) (CAS No. 335-67-1) and Perfluoro(2-methyl-3-oxahexanoic) acid (Gen-X) (CAS No. 13252-13-6) were purchased from Aladdin (Aladdin, Shanghai, China). Dulbecco's modified eagle medium (DMEM), Fetal bovine serum (FBS), Penicillin-Streptomycin (P/S), and Trypsin-EDTA (0.25%) with phenol red were purchased from Gibco (Gibco, NY, USA). Dimethyl sulfoxide (DMSO) was purchased from Solarbio (Solarbio, Beijing, China). 1M Tris pH 6.8 and 1M Tris pH 8.8 (Quayad, Beijing, China), Sodium Dodecyl Sulfate (SDS), Bovine Serum Albumin (BSA), Tris-base and Glycine (BioFroxx, Einhausen, Germany), Ammonium Persulfate (APS) and N,N,N',N'-Tetramethylethylenediamine (MACKIIN, Shanghai, China), Tween 20 (VETEC, Speyer, Germany), were used to make gels, running buffer and transferring buffer in Western blot. Methanol and Chloroform were purchased from Titan (Titan, Shanghai, China). PageRuler™ Prestained protein MW standard, 10 to 180 kDa (Thermo Fisher Scientific, MA, USA) was used as protein ruler. ECL WB substrate (Tanon, Shanghai, China) was used in protein imaging. Trizol was purchased from Sigma-Aldrich Corporation (St. Louis, MO, USA). DEPC water and RNase-free ddH<sub>2</sub>O were from Adamas life (Adamas life, Shanghai, China). Antibodies used in this study are listed as following, GAPDH Mouse mAb (Cell Signaling Technology, MA, USA), Phospho-Histone H2A.X Rabbit mAb (Cell Signaling Technology, MA, USA),

SMAD2 Rabbit mAb (Abcam, Cambridge, UK), SMAD4 Rabbit mAb (Abcam, Cambridge, UK), TGF $\beta$ <sub>3</sub> Rabbit mAb (Abcam, Cambridge, UK). Additional information can be found in **Appendix A**.

## **2.2. Cell culture maintenance**

To investigate the potential effects of PFOA and Gen-X on different organs in the human body, the present study used corresponding cell lines instead of human tissues for in vitro experiments. Four cell lines were used in this study, SN12C (human kidney cancer cell line, CL-0744), SW620 (human colon cancer cell line, CL-0225B), HepG2 (human liver cancer cell line, CL-0103), and A375 (human melanoma cell line, CL-0014). All cell lines were purchased from Procell Life Science&Technology Co., with correct STR identification. Cell culturing, cell passaging, cell freezing, and cell thawing were standardized according to the instructions accompanying each cell line. In addition, aseptic technique is critical to the maintenance of cell culture. All experiments were performed under standard aseptic conditions.

### **2.2.1. Cell culturing**

SN12C, SW620, HepG2, and A375 are adherent cells. All cells were cultured in T25 flasks (Corning, NY, USA, 430168) and transferred to T75 flasks (Corning, NY, USA, 3290) in the third generation. Typically, for cell culturing, 5 ml of complete medium is added to a T25 flask and 15 ml of complete medium is added to a T75 flask. The complete culture medium (CM-DMEM) is configured from 89% basic DMEM, 10%

FBS, and 1% P/S. After adding CM-DMEM, the flasks should be sterile and maintained in an incubator (Esco Micro Pte. Ltd., Singapore) at 37°C, CO<sub>2</sub> at 5%, pH at 7.4, and relative humidity at 95%. The color of the cell culture medium can be used as a qualitative indicator of pH. A hue close to yellow indicates a low pH and requires a change of medium or transfer of cells depending on the degree of cell confluence observed. If the medium change is required, new medium will need to be introduced after the old medium has been removed by pipetting.

### **2.2.2. Cell passaging**

When the cell confluence was observed under the microscope to reach about 80%, cell passaging could be performed. First the medium was removed, then the cells were washed three times 1mL with PBS. After removing the PBS with a pipette gun, 1 mL of trypsin (with EDTA) was added to a T25 flask or 2 ml of trypsin (with EDTA) to a T75 flask, followed by gentle shaking of the flask to penetrate all the cells. Cells were placed in the incubator for tryptic digest and the reaction was terminated once the cells in the middle of the cell block are clearly turned into circles with gaps under microscope by addition of 3 mL of CM-DMEM to T25, or 6 ml of CM-DMEM to T75 flasks. A single suspension was achieved by repeated aspiration of the resulting cell suspension, which was then transferred to a 15 mL centrifuge tube (Titan, Shanghai, China, SWLX-JZ015-ZX). The collected cell suspension was centrifuged with the centrifuge set at 1200 rpm/min for 3 minutes (Baiyang, Beijing, China), and the supernatant was pipetted out and discarded after centrifugation. Then, fresh CM-DMEM was added, and

cells were mixed by blowing for a few times. 1/3 of the cells were transferred to a new T25 or T75 flask and the medium was replenished to 5 ml in the T25 flask or 15 ml in the T75 flask. After gently shaking the flasks and labeling them appropriately, the flasks with cells were incubated in a sterilized incubator for further use. The medium should be changed the day after splitting the cells. All reagents are heated in a 37°C water bath before cell passaging.

### **2.2.3. Cell freezing**

The cell freezing process is similar to the cell passaging procedure. After centrifugation and removal of the supernatant, cells were resuspended by adding 1mL of freezing medium (55% basal medium, 40% FBS, 5% DMSO). The cell suspension was then counted under a microscope using a hemocytometer plate. Subsequently, the cell suspension was diluted to  $1 \times 10^6$  cells/mL and transferred to 2 mL cryotubes (Corning, NY, USA, 430659), 1 ml per tube. The cryotubes were placed in a cryo preservation cool-down box (Bioland, Zhejiang, China) in a -80° refrigerator overnight, and then transferred into liquid nitrogen until further use.

### **2.2.4. Cell thawing**

When thawing of cells is required, the frozen tubes are first removed from liquid nitrogen and placed in a 37°C water bath and shaken gently to thaw the cell suspension in the frozen tubes quickly. Subsequently, cells were transferred to a 2 mL centrifuge tube and then centrifuged at 1200 rpm for 5 minutes. The supernatant was pipetted using

a pipette gun and the cells were resuspended with 1 mL of CM-DMEM. Finally, the cells were transferred to a T25 flask and replenished to 5 mL with CM-DMEM, with gently shaking the flask and place the flask in the incubator.

### **2.3. Cell viability assay**

Cell viability was assessed using Enhanced Cell Counting Kit-8 (CCK-8) (Beyotime, Jiangsu, China, C0042) to establish the dose-response curves of each cell line to PFOA and GEN-X, facilitating subsequent experiments on PFOA and GENX exposure. Establishment of dose-response curves by CCK-8 assay can help to estimate the IC<sub>50</sub> of each cell line to PFOA and Gen-X for the study of subsequent toxicity studies on protein and gene expression.

#### **2.3.1. Cell plating**

The cell plating process is similar to the cell passaging process. After centrifugation and removal of the supernatant, 1 mL of CM-DMEM was added to resuspend the cells. The cell suspension was then counted under a microscope using a hemocytometer plate. Subsequently, the cell suspension was diluted to  $5 \times 10^5$  cells/mL and seeded into 96-well plates at 100  $\mu$ L per well with 3 replicate wells per group. The seeded 96-well plates were placed in an incubator for 24h. For cell plating in 6-well plates, 1 mL of cell suspension needs to be added per well and the medium is refilled to 2 mL per well using CM-DMEM.

### **2.3.2. Toxin exposure**

The cells were exposed to relevant toxic agents 24h after cell plating. First, the medium was removed from the 96-well plates. Subsequently, PFOA solution at concentrations of 0, 100, 250, 500, 750, and 1000  $\mu\text{M}$ , and GEN-X solution at concentrations of 0, 500, 1000, 2000, 3000, and 4000  $\mu\text{M}$  were added to each group. All PFOA and GEN-X solutions were made up from a pre-prepared stock solution. The stock solution of PFOA and GEN-X was prepared by dissolving in DMSO at the final concentration of 0.1M and 1M and kept at  $-20^{\circ}\text{C}$  (Abudayyak et al., 2021). The control group used complete medium containing 1% DMSO. All solutions were configured using complete medium as solvent and were prepared freshly.

### **2.3.3. CCK-8 assay**

After 48h of toxicity exposure, cell viability assay using CCK-8 was performed. 10  $\mu\text{L}$  of enhanced CCK-8 solution was added to each well, and the same 10  $\mu\text{L}$  of enhanced CCK-8 solution was added as a blank control in the control group where no cells were added. Incubation was continued for 2 h in a cell culture incubator, followed by measurement of absorbance at 450 nm using an enzyme-linked immunosorbent assay (ELISA) reader (Thermo Fisher Scientific, MA, USA).

## **2.4. Western blot**

The Western Blot protocol has been described in detail previously and will be outlined below (K. Hu et al., 2020). Certain steps were adapted to account for the variety of

antibodies applied in this study.

#### **2.4.1. Protein extraction**

First, the cells were spread into 6-well plates (NEST, Wuxi, China, 703003-ZX) for exposing to the concentrations of PFOA and Gen-X at 0 (CM-DMEM with 1% DMSO),  $1/2 IC_{50}$ ,  $IC_{50}$ ,  $2*IC_{50}$  for 48 hours. Then, RIPA Lysis Buffer was used to lyse the cells and extract the proteins. Thaw the RIPA lysate and mix well. Take the appropriate amount of lysis buffer and add PMSF within minutes before use so that the final concentration of PMSF is 1 mM. Remove the culture medium, wash the cells in 6-well plates with cold PBS, and add the RIPA lysis buffer at 200  $\mu$ L per well. Aspirate several times with a pipette gun to make full contact between the lysate and the cells. The 6-well plate was placed on ice for 10 minutes to allow for complete cell lysis followed by transfer of lysates to 1.5 mL centrifuge tubes and centrifugation at 12,000x-g for 5 min. The supernatant containing extracted proteins was then stored at -80°C.

#### **2.4.2. Sample preparation**

Total protein concentration was determined using the Enhanced BCA Protein Assay Kit (Beyotime, Jiangsu, China, P0009). The proteins and deionized water were mixed to make sure each sample at the same concentration with a total of 20  $\mu$ L or 30  $\mu$ L. 5  $\mu$ L of 5x SDS-PAGE Sampling Buffer was then added to each sample, followed by vortex, and incubating at 100 °C for 5 min. The heated samples were placed in a centrifuge and centrifuged at 1,000x-g for 10 seconds, ensuring that the walls of the centrifuge tubes

were free of water vapor.

### **2.4.3.SDS-PAGE**

In order to perform SDS-PAGE, 10% and 15% gels (Appendix B) were prepared using a gel casting system (Tanon, Shanghai, China) and stored overnight in a refrigerator at 4°C. The gels were made with 10 sampling wells each, with a 1.5 mm thickness, which could contain 25 to 35  $\mu$ L of sample per well. In addition, protein ladders (10-180 kDa) were loaded as a reference. Gel electrophoresis was performed in running buffer (Appendix B) with gel electrophoresis system (Tanon, Shanghai, China), starting at 90 V for 30 min followed with 120 V for 60 min until the blue dye was near the bottom of the gel.

### **2.4.4.Membrane transferring**

At the end of gel electrophoresis, the electrophoretically separated proteins were transferred to a PVDF membrane (MilliporeSigma, MA, USA). First, the PVDF membrane was cut to the same size as the gel and put into methanol to activate for 1 min. Subsequently, the activated PVDF membrane was attached to the gel, ensuring that there were no bubbles between the two. The gel was placed in the negative electrode and the PVDF membrane was placed in the positive electrode, and a sponge and two pieces of filter paper were placed sequentially between the electrode plate and the gel and PVDF membrane, respectively. The stack was then put into the wet transfer system (Tanon, Shanghai, China) by addition of transfer buffer (Appendix B). The

whole transfer system was placed on ice, which was running under 315 mA for 1.5h.

#### **2.4.5.Blocking**

The transferred PVDF membrane was cut around the molecular weights of the target proteins with the reference of protein ladder (GAPDH: 37 kDa, Smad2: 60 kDa, Smad4: 60-65 kDa, H2A.X: 15 kDa, TGF  $\beta$ 3: 47-55 kDa). The cut PVDF membranes were placed in a WB incubation box and blocked on an orbital shaker for 1h at room temperature by adding blocking buffer (5% BSA dissolved in TBST, Appendix B). Subsequently, the blocking buffer was recycled followed by washing membranes three times with TBST for 5 min .

#### **2.4.6.Primary antibody incubation**

The primary antibodies were diluted using 1% BSA (dissolved in TBST) solution (GAPDH: 1:1000, Smad2: 1:2000, Smad4:1:5000, H2A.X: 1:1000, TGF  $\beta$ 3: 1:1000). The diluted primary antibody solution was added to the WB incubation box and incubated at 4°C cold room overnight.

#### **2.4.7.Secondary antibody incubation**

The primary antibody was recycled, and the membrane was subsequently washed three times using TBST for 10 min each time. Goat anti-rabbit and goat anti-mouse antibodies which diluted in 1% BSA solution (1:5000) were used as secondary antibodies followed by incubating for 1.5h at room temperature on an orbital shaker. After incubation, the

membrane was washed again with TBST three times for 5 min each.

#### **2.4.8. Protein Imaging**

The membranes were covered with freshly mixed ECL solution and examined in a pre-cooled chemiluminescence imaging system (Bio-Rad Laboratories, CA, USA). Photographs of the proteins were taken after the membranes were exposed for a certain time in UV mode.

#### **2.5. RNA extraction**

Total RNA extraction using Trizol reagent has been described in detail in previous researches and will be outlined below (Gandhi et al., 2020). First, the cells were spread into 6-well plates and exposed to the cells at concentrations of 0 (CM-DMEM with 1% DMSO),  $1/2 IC_{50}$ ,  $IC_{50}$ ,  $2*IC_{50}$  for 48 hours. Subsequently, culture solution was aspirated and 1 mL of Trizol was added to each well of a 6-well plate followed by gentle shaking 3-5 times and pipette 2-3 times to ensure complete lysis. The lysis buffer with sample was then aspirated into a centrifuge tube and leaved at room temperature for 5 minutes to allow the sample to fully lysis. 0.2 mL of chloroform per mL of Trizol was added followed by shaking vigorously for 15 seconds. Leaving the sample at room temperature for 2-3 minutes. The sample was centrifuged at 12,000x-g for 15 minutes at 4°C. The upper colorless aqueous phase containing the total RNA was aspirated into a new centrifuge tube. Subsequently, 0.5 ml of isopropanol was added per mL of initial Trizol, followed by mixing several times by inversion, and precipitated for 10 min at

room temperature. Centrifugation was performed at 12,000x-g 4°C for 10 min, after which the RNA precipitate was visible at the bottom of the tube and discarded the supernatant. 1 mL of 75% ethanol (prepared in DEPC water) was added per mL of initial Trizol with inverted mixing. Centrifugation was performed at 7,500x-g for 5 min at 4°C and the supernatant was discarded after centrifugation. Centrifuging again at 5,000x-g for 5 seconds and carefully aspirating the remaining liquid. 20 µL of DEPC water was added to dissolve the sample after the RNA dried slightly. The DEPC water containing extracted total RNA was then stored at -80°C.

## **2.6. cDNA Synthesis**

The HiScript II 1st Strand cDNA Synthesis Kit (Vazyme, Nanjing, China) was used for cDNA synthesis. First, the concentration of extracted RNA was assayed using nanodrop (Thermo Fisher Scientific, MA, USA). The first-strand cDNA synthesis reaction solution was configured in RNase-free centrifuge tubes, and the mass of total RNA per sample was ensured to be 1 µg by calculation. The reaction solution was mixed by gently blowing with a pipette and sequentially reacted at 25°C for 5 min, 50°C for 15 min, and 85°C for 2 min in a PCR thermal cycler (Bio-Rad Laboratories, CA, USA). The products were stored at -20°C.

## **2.7. RT-PCR**

RT-qPCR experiments were performed using 96-well PCR plates (NEST, Wuxi, China). In the 20 µL reaction system, 10 µL was ChamQ Universal SYBR qPCR Master Mix

(Vazyme, Nanjing, China), 0.4  $\mu\text{L}$  of 1  $\mu\text{M}$  forward primer, 0.4  $\mu\text{L}$  of 1  $\mu\text{M}$  reverse primer, 7.2  $\mu\text{L}$  of RNase-free ddH<sub>2</sub>O, and 2  $\mu\text{L}$  of template cDNA. All primers were synthesized by AZENTA Life Sciences (Suzhou, China), details are shown in **Appendix A**. The RT-qPCR thermal cycler (Bio-Rad Laboratories, CA, USA) was set as 95°C for 30 seconds with 1 repetition (Pre-denaturation), 95°C 10 seconds and 60°C 30 seconds with 40 repetitions (Cycling Reactions), and a melting curve acquisition (Default melting curve program).

## **2.8. Statistical analysis**

The results are presented as mean  $\pm$  standard deviation (SD). Data from the experiments were analyzed by ANOVA using GraphPad Prism version 9.5.1 for Windows (GraphPad Software, San Diego, CA). P-value < 0.05 was considered significant.

## Chapter 3: Results

### 3. Results

#### 3.1. Cytotoxicity assessment

In this study, the cytotoxic effects of PFOA and Gen-X were systematically evaluated in four different human cancer cell lines (A375, SN12C, HepG2, SW620), these cell lines cover the major pathways of PFOA and Gen-X exposure and accumulation in vivo. This study analyzed the effects of PFOA and Gen-X on cellular gene expression in vitro by Western blot, and RT-PCR. In order to confirm the drug resistance of each cell line to PFOA and Gen-X, the CCK-8 cytotoxicity assay was first performed in this study, and the half inhibitory concentration ( $IC_{50}$ ) of each cell line was estimated by a nonlinear regression model, which facilitates the subsequent exposure toxicity study. Table 1 demonstrates the estimation results of the non-linear regression model.

##### 3.1.1. A375 cell line

The skin-derived melanoma A375 cell line, showed a high sensitivity to PFOA with an  $IC_{50}$  value of 213.2  $\mu$ M (nonlinear regression  $R^2 = 0.9375$ ) (Fig. 1A), indicating that this compound significantly inhibits cell survival even at relatively low concentrations. On the other hand, the same cell line was significantly more tolerant to Gen-X, cell viability began to show a significant decrease after a 500  $\mu$ M concentration of Gen-X, with an  $IC_{50}$  value of up to 1555  $\mu$ M (nonlinear regression  $R^2 = 0.9920$ ) (Fig. 2A). This suggests that the two compounds may affect the survival of A375 cells through different

mechanisms or with different intracellular targets, which will be analyzed further in the discussion.

### **3.1.2. SN12C cell line**

The kidney cancer cell line SN12C was the most resistant to PFOA with an  $IC_{50}$  value of 616.3  $\mu\text{M}$  (nonlinear regression  $R^2 = 0.9684$ ) (Fig. 1B). For Gen-X, the tolerance of SN12C cells further increased with  $IC_{50}$  values up to 5048  $\mu\text{M}$  (nonlinear regression  $R^2 = 0.9400$ ) (Fig. 2B), which exceeded the maximum of the concentration gradient set for the study and was the highest in the study. In addition, it can be also observed in Fig. 2B that SN12C cells showed higher proliferation under exposure to lower concentrations of Gen-X ( $<1000 \mu\text{M}$ ).

### **3.1.3. SW620 cell line**

The SW620 cell line derived from colon cancer showed moderate sensitivity to PFOA with an  $IC_{50}$  of 271.2  $\mu\text{M}$  (nonlinear regression  $R^2 = 0.9965$ ) (Fig. 1C). For Gen-X, SW620 also showed moderate tolerance with an  $IC_{50}$  of 2126  $\mu\text{M}$  (nonlinear regression  $R^2 = 0.9874$ ) (Fig. 2C).

### **3.1.4. HepG2 cell line**

HepG2, as liver cancer cells, showed moderately low sensitivity to PFOA with an  $IC_{50}$  of 527.9  $\mu\text{M}$  (nonlinear regression  $R^2 = 0.9974$ ) (Fig. 1D), consistent with the role of the liver in metabolism and detoxification processes. The tolerance of the cells was

further increased by Gen-X exposure with an  $IC_{50}$  of 2377  $\mu\text{M}$  (nonlinear regression  $R^2 = 0.9747$ ) (Fig. 2D).

**Table 1:  $IC_{50}$  (with 95% confidence intervals) of A375, SN12C, SW620, and HepG2 cells in response to PFOA and Gen-X, obtained by CCK-8 assay, were estimated by fitting the results using nonlinear regression.**

Cell lines	PFOA treated $IC_{50}$ $\mu\text{M}$ (95% CI)	Gen-X treated $IC_{50}$ $\mu\text{M}$ (95% CI)
A375	213.2 (23.54, 393.8)	1555 (1452, 1664)
SN12C	616.3 (558.8, 670.1)	5048 (4451, 6193)
SW620	271.2 (239.8, 304.4)	2126 (1984, 2267)
HepG2	527.9 (??*, 541.2)	2377 (2148, 2630)

\* Unable to estimate specific values

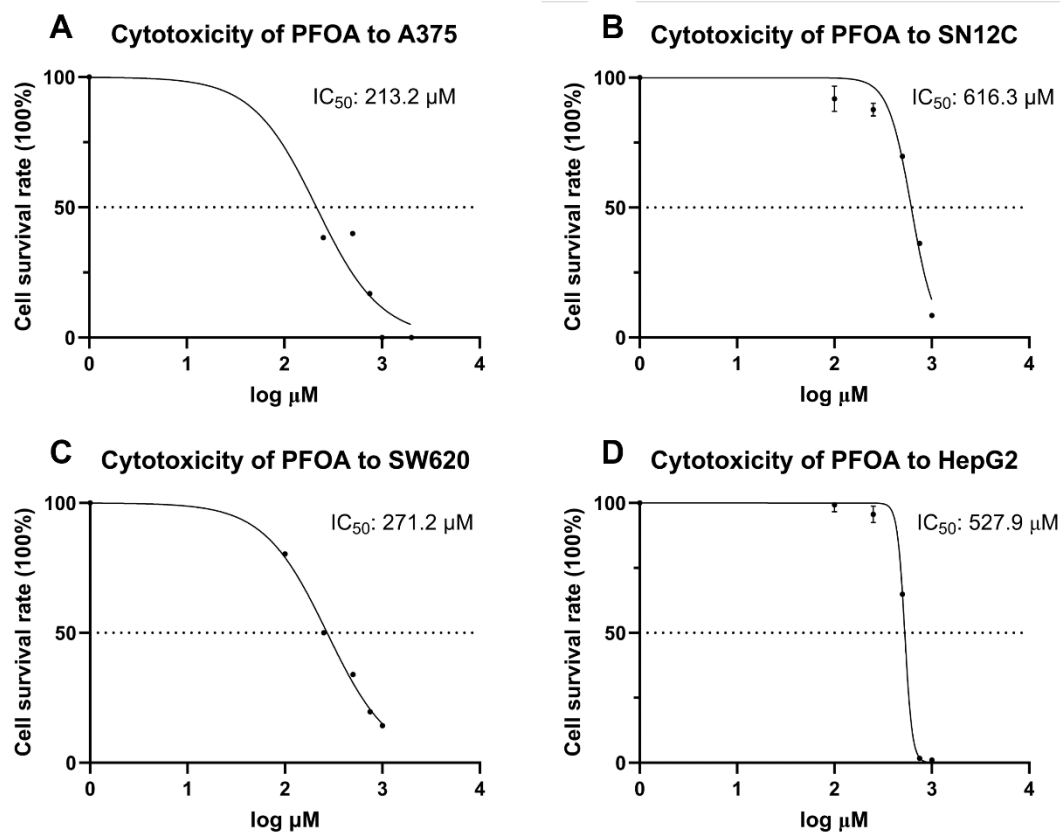


**Figure 1: Viability of (A) A375, (B) SN12C, (C) SW620, (D) HepG2 cells exposed to PFOA by CCK-**

**8 assay.** The data obtained through CCK-8 experiments were transformed to a log base after processing, fitted using nonlinear regression, and resulted in cell viability curves for each cell in response to PFOA concentration. Dashed lines represent the PFOA concentration at which half of the cells survived ( $IC_{50}$ ), and the best-fit values are labeled in the upper right corner. DMSO was used as a solvent for all PFOA group.

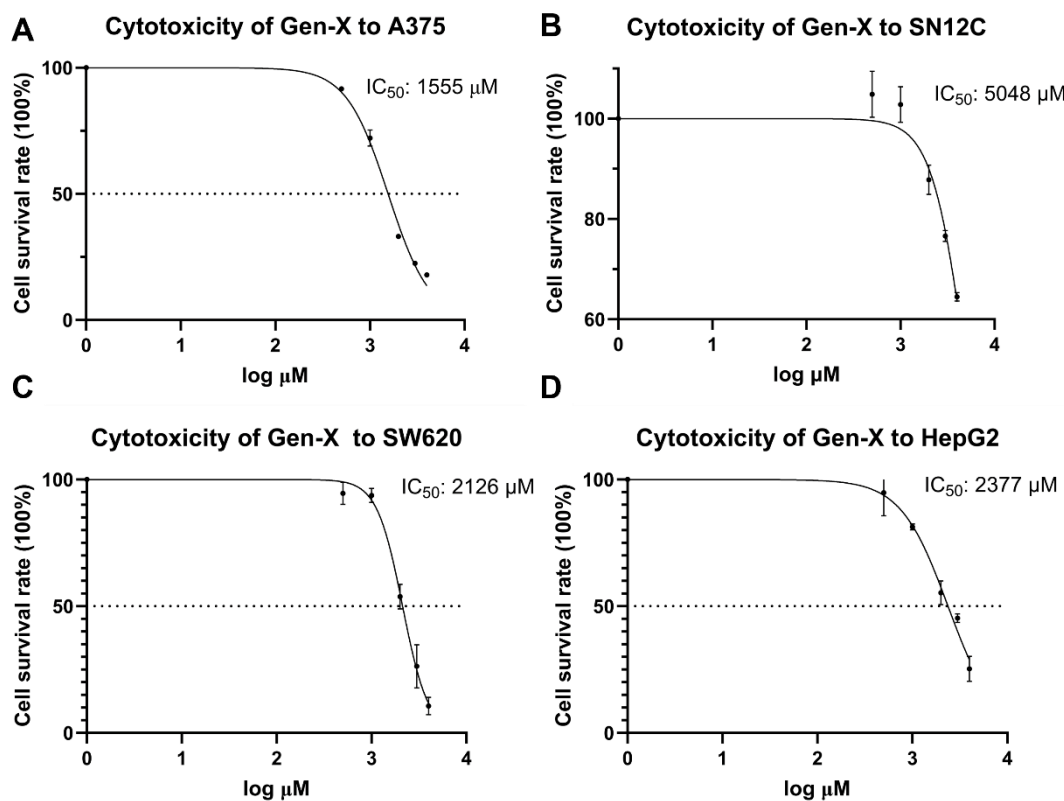


**Figure 2: Viability of (A) A375, (B) SN12C, (C) SW620, (D) HepG2 cells exposed to Gen-X by CCK-8 assay.** The data obtained through CCK-8 experiments were transformed to a log base after processing, fitted using nonlinear regression, and resulted in cell viability curves for each cell in response to Gen-X concentration. Dashed lines represent the Gen-X concentration at which half of the cells survived ( $IC_{50}$ ), and the best-fit values are labeled in the upper right corner. DMSO was used as a solvent for all Gen-X group.

### 3.2. Protein expression results

Having established that Gen-X and PFOA negatively affect cell growth and survival, the associated molecular pathways have become a new focus of research. Therefore, we performed western blotting experiments on PFOA- and Gen-X-treated A375, SN12C, HepG2, and SW620 cells to explore the response of the TGF- $\beta$  pathway, TGF $\beta_3$ , SMAD2, and SMAD4, to PFOA and Gen-X exposure. In addition, the abundance of  $\gamma$ -

H2AX will be examined to assess the potential damage to DNA by exposure to the target compounds.

### 3.2.1. Abundance of $\gamma$ -H2A.X

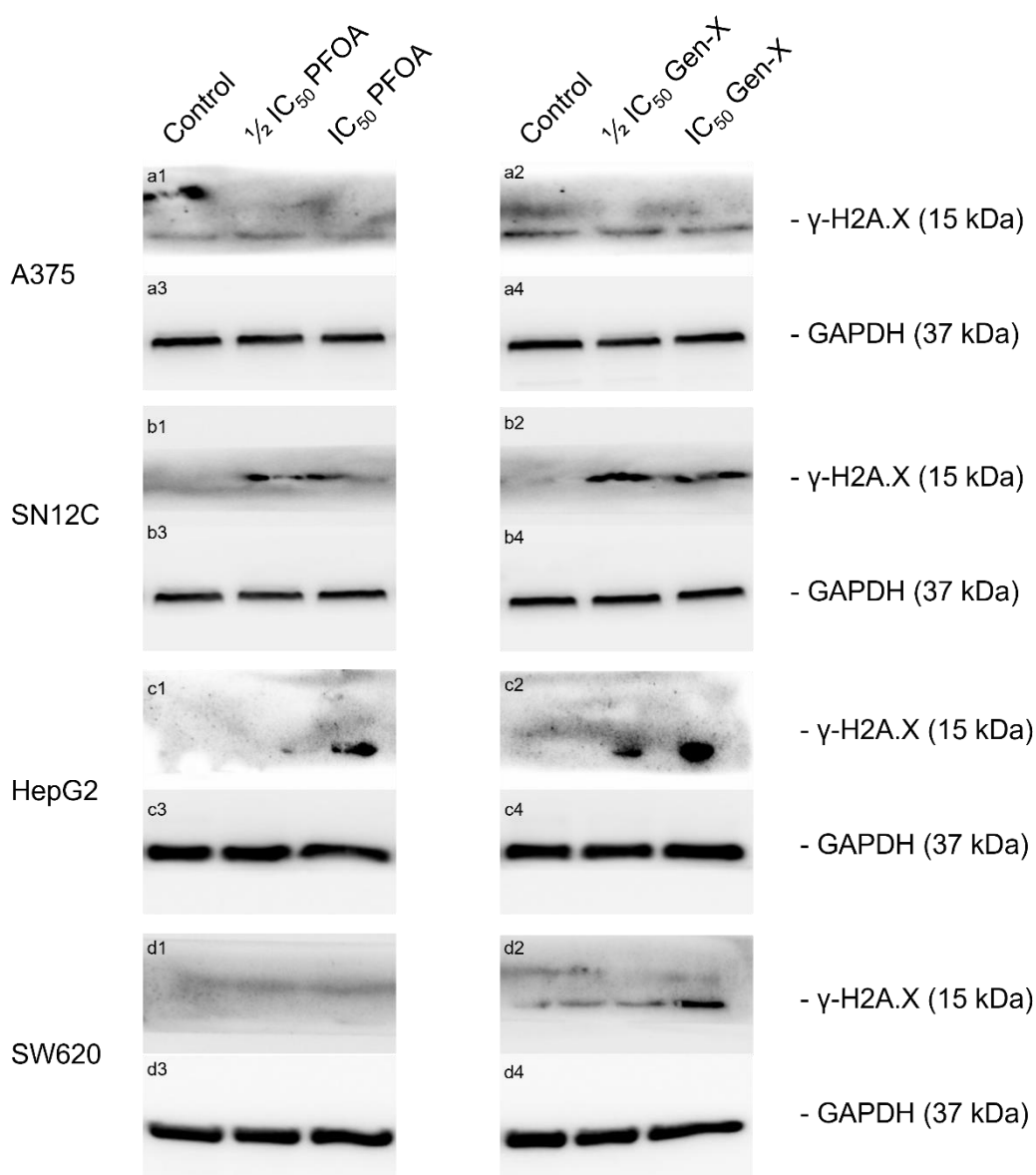


**Figure 3: Western blot analysis of abundance of  $\gamma$ -H2A.X (15 kDa) in (a) A375, (b) SN12C, (c) HepG2, (d) SW620 exposed by PFOA (a1, b1, c1, d1) with loading control GAPDH (37 kDa) (a3, b3, c3, d3) and by Gen-X (a2, b2, c2, d2) with loading control GAPDH (37 kDa) (a4, b4, c4, d4). The lanes of each plot represent, from left to right, the Control, the 1/2 IC<sub>50</sub> concentration target compound, and the IC<sub>50</sub> concentration target compound, respectively.**

It can be observed from Figure 3 that the overall abundance of  $\gamma$ -H2A.X increased with

increasing drug concentration. In the A375 cell line, it was observed that  $\gamma$ -H2A.X was expressed in all groups, but there was no clear trend (Fig. 3 a1 a2). In the SN12C cell line,  $\gamma$ -H2A.X cannot be observed in the control group and the abundance increased gradually with the increase of PFOA and Gen-X exposure (Fig. 3 b1 b2). The abundance trend of HepG2 was similar to that of SN12C (Fig. 3 c1 c2). In the SW620 cell line, the abundance of  $\gamma$ -H2A.X increased with the increase of the concentration in the Gen-X exposed group (Fig. 3 d2). In the PFOA group, there was no significant abundance of  $\gamma$ -H2A.X (Fig. 3 d1).

### **3.2.2. Pathway analysis of PFOA and Gen-X impact**

In order to investigate the effects of PFOA and Gen-X exposure on the signaling pathways in the four cancer cell lines, in addition to using western blotting experiments to detect changes in protein expression within the pathway, RT-PCR experiments were also conducted to examine the genes within the TGF- $\beta$  signaling pathway, TGF $\beta$ <sub>1</sub>, TGF $\beta$ <sub>2</sub>, TGF $\beta$ <sub>3</sub>, SMAD1, SMAD2, SMAD3, SMAD4, and p53 expression were examined. In addition, the expression of genes ATM/ATR, RPL5/11, which are related to DNA damage and repair mechanisms, were also examined to further understand the mechanism of cellular response to PFOA and Gen-X exposure.

The mRNA expression levels of the target genes in each cell line of each experimental group were evaluated using real-time quantitative polymerase chain reaction (RT-PCR). Relative expression was calculated using the  $2^{-\Delta\Delta C_t}$  method, and differences in expression between groups were analyzed for significance using ANOVA analysis

(three groups of data) or t-test (two groups of data). \*,  $p < 0.05$ ; \*\*,  $p < 0.01$ , \*\*\*  $p < 0.001$ .

### **3.2.3.Expression from A375 cell line**

The right panels of Figure 4 demonstrate the protein expression levels of the A375 cell line after PFOA treatment. In particular, the expression level of SMAD4 showed an increasing trend with increasing PFOA concentration, while no significant trend could be observed for the expression of other proteins. The right panels of Figure 5 demonstrate the protein expression levels of the A375 cell line after Gen-X treatment. The expression level of TGF $\beta_3$  showed a decreasing trend with increasing Gen-X concentration, and no significant trend could be observed for the expression of other proteins.

As shown in left panels of Figure 4, significant changes in the expression of certain genes such as TGF $\beta_1$ , SMAD2, p53, and RPL11 were observed at IC<sub>50</sub> and  $\frac{1}{2}$  IC<sub>50</sub> concentrations of PFOA as compared to untreated controls in A375 cell line. The expression of TGF $\beta_1$  was decreased at  $\frac{1}{2}$  IC<sub>50</sub> concentration compared to the control, while it was increased at IC<sub>50</sub> concentration, but the change was not significant. Meanwhile, SMAD2 and SMAD4 exhibited significant up-regulation at IC<sub>50</sub> concentrations ( $p < 0.05$  and  $p < 0.001$ , respectively), suggesting that these signaling pathways may play a key role in cellular response to PFOA. It is notable that p53 and ATR also showed significant up-regulation at IC<sub>50</sub> concentration ( $p < 0.001$ ), suggesting that DNA damage response may be activated. In addition, the expression of the

ribosomal protein gene RPL11 was significantly increased at IC<sub>50</sub> concentration ( $p < 0.001$ ), which may reflect the protein synthesis stress of cells under PFOA exposure. However, the expression of other genes such as TGF $\beta$ <sub>2</sub>, TGF $\beta$ <sub>3</sub>, SMAD1 and SMAD3 did not change significantly in the experimental group.

Significant gene expression changes were also observed in the Gen-X treated group (Fig. 5). In the TGF- $\beta$  family genes, TGF $\beta$ <sub>1</sub> gene expression decreased at IC<sub>50</sub>-treated concentrations ( $p < 0.001$ ), and the expression of TGF $\beta$ <sub>3</sub> increased significantly at both  $\frac{1}{2}$  IC<sub>50</sub> and IC<sub>50</sub> concentrations ( $p < 0.05$  and  $p < 0.001$ ), while TGF $\beta$ <sub>2</sub> did not show a corresponding signal in the experiment (N/A). In the SMAD family genes, SMAD1, SMAD3 and SMAD4 showed significant up-regulation at IC<sub>50</sub> concentrations ( $p < 0.001$  for SMAD1, SMAD3 and  $p < 0.05$  for SMAD4), which is consistent with the activation of the TGF- $\beta$  signaling pathway. However, the expression of SMAD2 did not show statistically significant changes after Gen-X treatment. In addition, ATM also showed a significant increase in expression at IC<sub>50</sub> concentrations ( $p < 0.01$ ), suggesting that a DNA damage response mechanism may have been induced in the presence of Gen-X. However, the p53 gene showed a significant decrease in expression at IC<sub>50</sub> concentration ( $p < 0.05$ ).

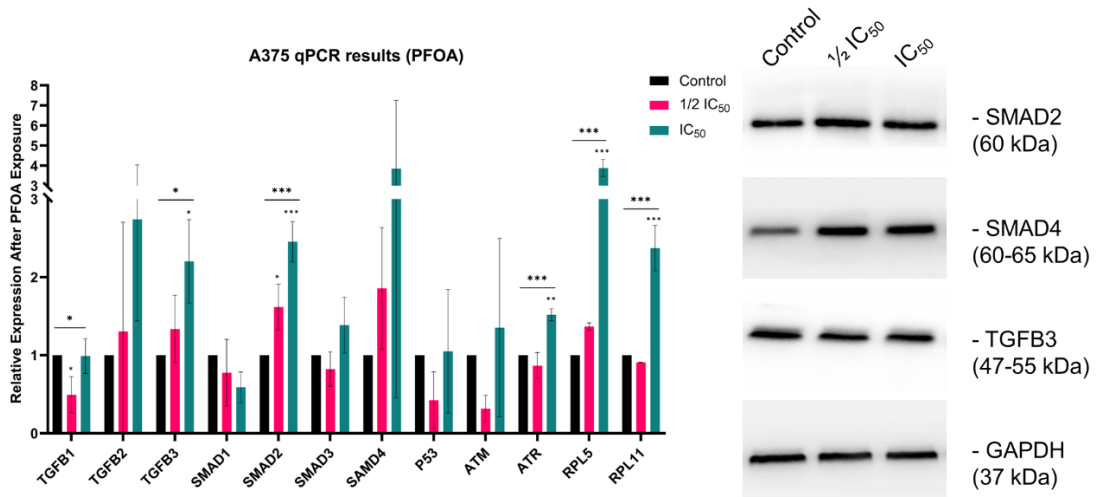


**Figure 4: Altered gene expression (left) and protein expression (right) in A375 cells following exposure to PFOA.** A375 cells were either mock-treated, or treated with PFOA with concentration of 1/2 IC<sub>50</sub>, IC<sub>50</sub> for 48 h, and then the relative mRNA levels were determined by RT-PCR. Data shown are mean ± SD of three independent experiments. \*, p < 0.05; \*\*, p < 0.01, \*\*\* p < 0.001. The lanes of each plot on the right panel represent, from left to right, the Control, the 1/2 IC<sub>50</sub> concentration target compound, and the IC<sub>50</sub> concentration target compound, respectively.

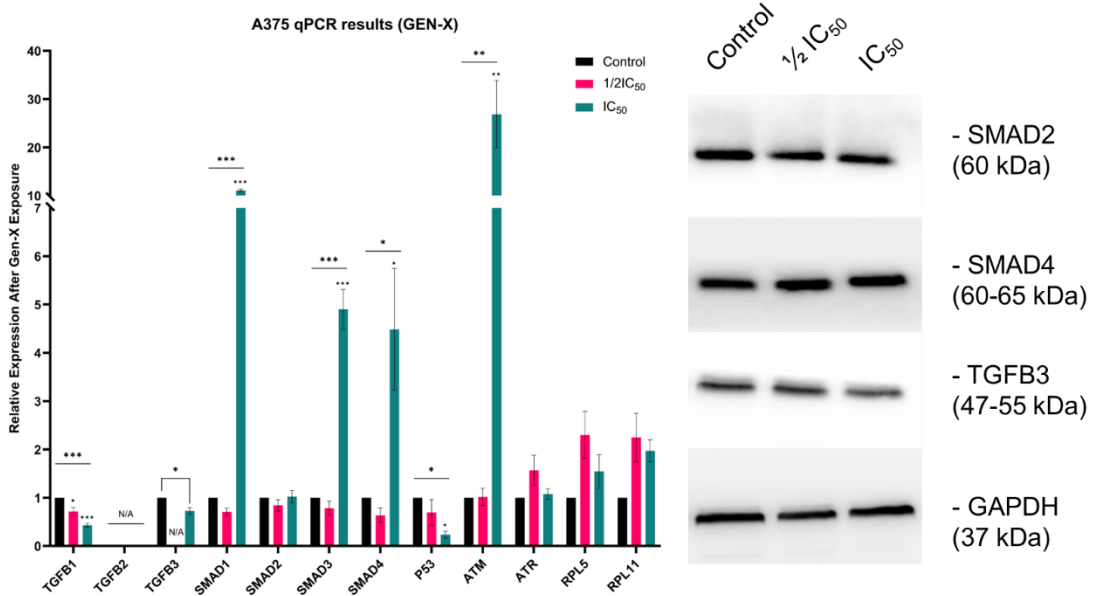


**Figure 5: Altered gene expression (left) and protein expression (right) in A375 cells following exposure to Gen-X.** A375 cells were either mock-treated, or treated with Gen-X with concentration of 1/2 IC<sub>50</sub>, IC<sub>50</sub> for 48 h, and then the relative mRNA levels were determined by RT-PCR. Data shown are mean ± SD of three independent experiments. \*, p < 0.05; \*\*, p < 0.01, \*\*\* p < 0.001. The lanes of each plot on the right panel represent, from left to right, the Control, the 1/2 IC<sub>50</sub> concentration target compound, and the IC<sub>50</sub> concentration target compound, respectively.

### 3.2.4.Expression from SN12C cell line

The right panels of Figure 6 illustrate the variations in protein expression within the SN12C cell line after treatment with PFOA, where a negative correlation between TGF $\beta$ <sub>3</sub> expression and PFOA concentration is observed. In contrast, the right panels of Figure 7 present the alterations in protein expression following Gen-X administration, showcasing an upward trend in SMAD2 levels concomitant with increasing Gen-X concentrations. Moreover, the expression levels of SMAD4 and TGF $\beta$ <sub>3</sub> demonstrate a decreasing trend in response to escalating Gen-X concentrations.

The left panels of Figure 6 demonstrates the gene expression differences in SN12C cell line after PFOA treatment. The expression of TGF $\beta$ <sub>1</sub>, TGF $\beta$ <sub>2</sub>, and TGF $\beta$ <sub>3</sub>, as well as the signaling molecules associated with them (SMAD1, SMAD2, SMAD3, and SMAD4), was significantly decreased after treatment with both the  $\frac{1}{2}$  IC<sub>50</sub> and IC<sub>50</sub> concentrations of PFOA, and the expression of these genes was particularly more pronounced at IC<sub>50</sub> concentrations, with the statistical significance reaching the level of  $p < 0.001$ . Similarly, the expression of genes p53, ATM, and ATR, which are associated with cellular stress response and DNA damage repair mechanisms, was significantly decreased after PFOA treatment. The ribosomal protein genes RPL5 and RPL11 also showed reduced expression under the influence of PFOA, especially at IC<sub>50</sub> concentrations, which may reflect disturbed protein synthesis in cells under chemical stress.

In the Gen-X treatment group (Fig. 7), the situation was different. The genes of the TGF- $\beta$  family, TGF $\beta$ <sub>1</sub> and TGF $\beta$ <sub>3</sub>, showed a decrease in expression at  $\frac{1}{2}$  IC<sub>50</sub> and IC<sub>50</sub> concentrations, with TGF $\beta$ <sub>3</sub> showing a more significant decrease at IC<sub>50</sub> concentrations

( $p < 0.001$ ), and  $TGF\beta_2$  showing an increase in expression, but lacking statistical significance. Genes of the SMAD family showed a similar expression pattern after Gen-X treatment, with a significant increase in expression at  $IC_{50}$  concentration ( $p < 0.001$ ). Meanwhile, the expression of p53, ATM and ATR was significantly increased at  $IC_{50}$  concentration ( $p < 0.001$ ), and the expression of RPL5 and RPL11 was also significantly increased under Gen-X treatment ( $p < 0.001$ ).

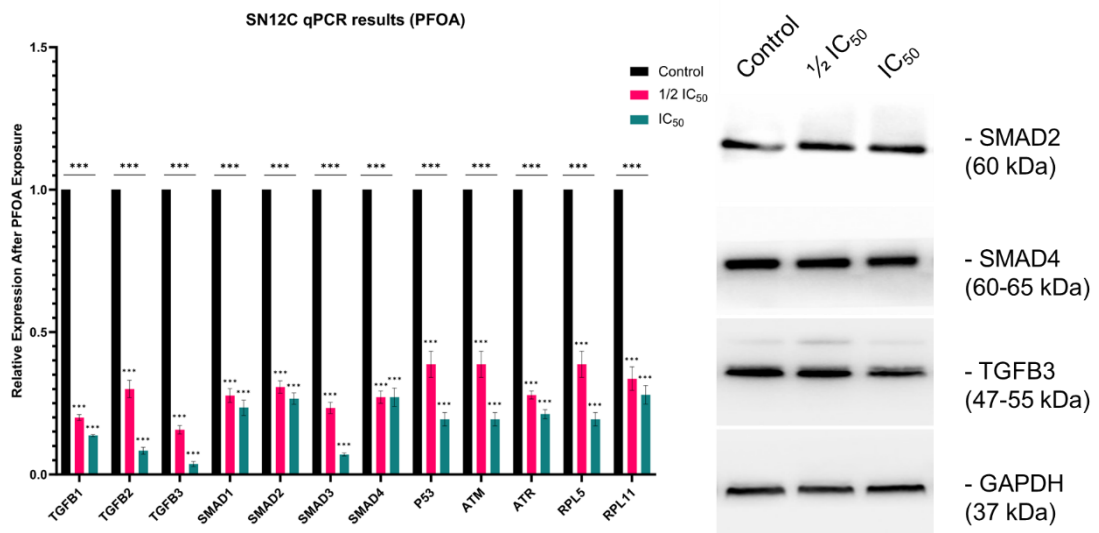


**Figure 6: Altered gene expression (left) and protein expression (right) in SN12C cells following exposure to PFOA.** SN12C cells were either mock-treated, or treated with PFOA with concentration of  $1/2 IC_{50}$ ,  $IC_{50}$  for 48 h, and then the relative mRNA levels were determined by RT-PCR. Data shown are mean  $\pm$  SD of three independent experiments. \*,  $p < 0.05$ ; \*\*,  $p < 0.01$ , \*\*\*  $p < 0.001$ . The lanes of each plot on the right panel represent, from left to right, the Control, the  $1/2 IC_{50}$  concentration target compound, and the  $IC_{50}$  concentration target compound, respectively.

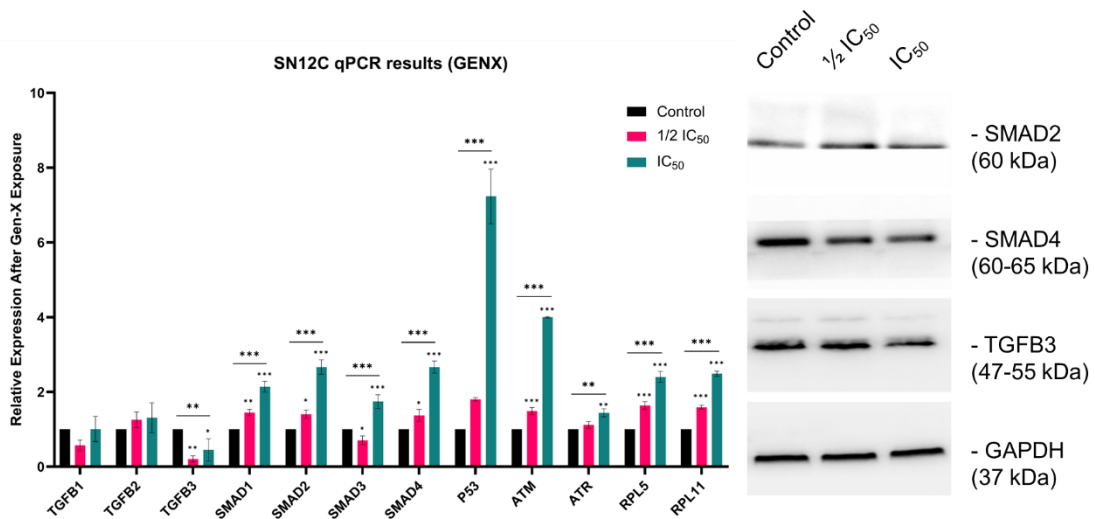


**Figure 7: Altered gene expression (left) and protein expression (right) in SN12C cells following exposure to Gen-X.** SN12C cells were either mock-treated, or treated with Gen-X with concentration of 1/2 IC<sub>50</sub>, IC<sub>50</sub> for 48 h, and then the relative mRNA levels were determined by RT-PCR. Data shown are mean ± SD of three independent experiments. \*, p < 0.05; \*\*, p < 0.01, \*\*\* p < 0.001. The lanes of each plot on the right panel represent, from left to right, the Control, the 1/2 IC<sub>50</sub> concentration target compound, and the IC<sub>50</sub> concentration target compound, respectively.

### 3.2.5. Expression from HepG2 cell line

The right panels of Figure 8 demonstrate the protein expression levels of the HepG2 cell line after PFOA treatment. The expression levels of SMAD2, SMAD4 and TGFβ<sub>3</sub> showed a decreasing trend with increasing PFOA concentration. The right panels of Figure 9 show the protein expression levels of the HepG2 cell line after Gen-X treatment. The expression levels of SMAD2 showed a decreasing trend with increasing Gen-X concentration, and no significant trend could be observed for the expression of other proteins.

The left panels of Figure 8 demonstrate the gene expression differences in HepG2 cell line after PFOA treatment. The results showed that the expression of the TGFβ<sub>1</sub> gene was significantly higher in the IC<sub>50</sub> group than in the control group, exhibiting an

approximately 6-fold increase ( $p < 0.001$ ), whereas the expression of this gene also rose in the  $1/2$   $IC_{50}$  group, but to a lower extent. For  $TGF\beta_3$ , although an upward trend in expression was observed in the  $IC_{50}$  group ( $p < 0.001$ ), however, there was a significant decrease in gene expression at  $1/2$   $IC_{50}$  concentrations. The expression data for  $TGF\beta_2$  were not applicable to this analysis (N/A). Some of the SMAD family genes also showed significant changes in expression levels in response to PFOA. SMAD2, SMAD3 and SMAD4 genes showed a significant increase in expression in the  $IC_{50}$  group ( $p < 0.001$ ). SMAD1 did not show any significant changes in either the  $1/2$   $IC_{50}$  or  $IC_{50}$  groups. In addition, the expression of cell cycle regulatory gene p53 and DNA repair genes ATM and ATR were significantly increased in the  $IC_{50}$  group. The expression of the ribosomal protein gene RPL5 was significantly higher in the  $IC_{50}$  group, while RPL11 expression was not significantly different in all groups.

In the Gen-X treatment group (Fig. 9), all target genes expression showed increases in different degrees. It is worth noting that both  $TGF\beta_1$ ,  $TGF\beta_2$  showed more than 20-fold gene expression at  $IC_{50}$  concentration. The SMAD1 gene showed great expression increase at the  $1/2$   $IC_{50}$  concentration, but the increase at the  $IC_{50}$  concentration did not exhibit statistical significance. In terms of cell cycle regulatory genes, the expression of P53 was significantly increased in the  $IC_{50}$  group, while the expression of the DNA damage response genes ATM and ATR was also significantly increased in the  $IC_{50}$  group. Ribosomal protein genes RPL5 and RPL11 also showed a significant increase in expression in the  $IC_{50}$  group, suggesting a possible perturbation of the protein synthesis process.

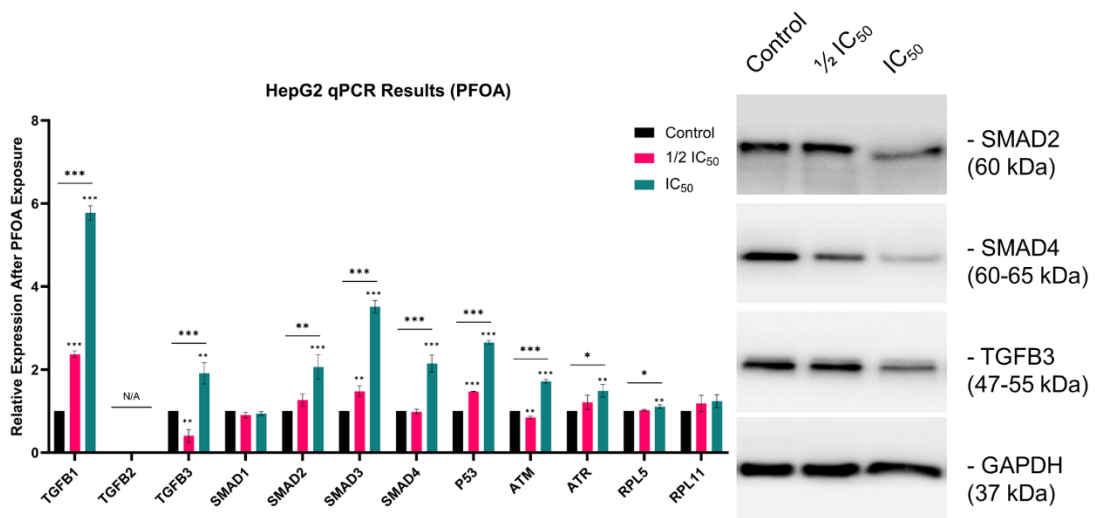


**Figure 8: Altered gene expression (left) and protein expression (right) in HepG2 cells following exposure to PFOA.** HepG2 cells were either mock-treated, or treated with PFOA with concentration of 1/2 IC<sub>50</sub>, IC<sub>50</sub> for 48 h, and then the relative mRNA levels were determined by RT-PCR. Data shown are mean ± SD of three independent experiments. \*, p < 0.05; \*\*, p < 0.01, \*\*\* p < 0.001. The lanes of each plot on the right panel represent, from left to right, the Control, the 1/2 IC<sub>50</sub> concentration target compound, and the IC<sub>50</sub> concentration target compound, respectively.

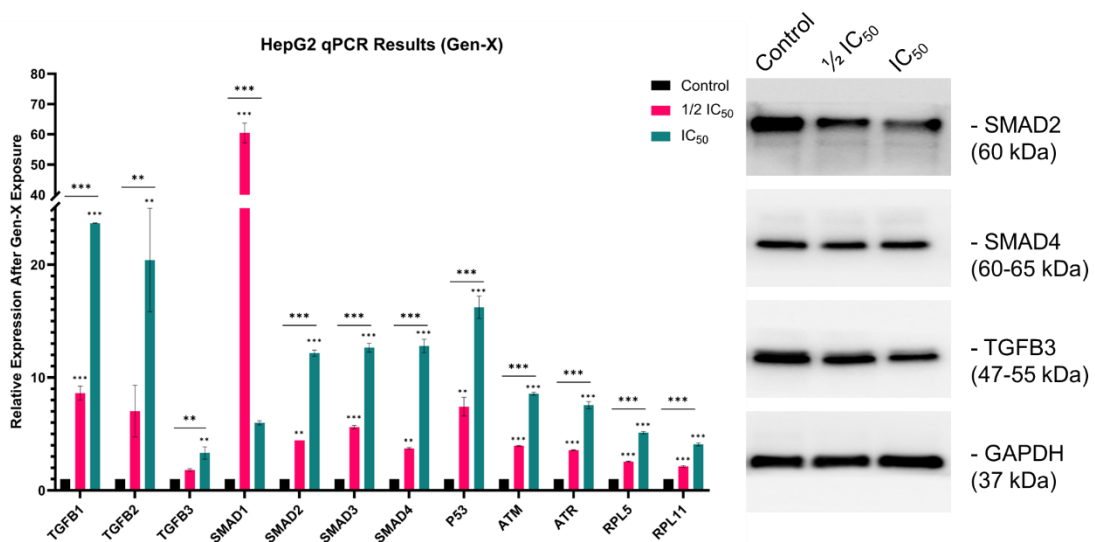


**Figure 9: Altered gene expression (left) and protein expression (right) in HepG2 cells following exposure to Gen-X.** HepG2 cells were either mock-treated, or treated with Gen-X with concentration of 1/2 IC<sub>50</sub>, IC<sub>50</sub> for 48 h, and then the relative mRNA levels were determined by RT-PCR. Data shown are mean ± SD of three independent experiments. \*, p < 0.05; \*\*, p < 0.01, \*\*\* p < 0.001. The lanes of each plot on the right panel represent, from left to right, the Control, the 1/2 IC<sub>50</sub> concentration target compound, and the IC<sub>50</sub> concentration target compound, respectively.

### 3.2.6.Expression from SW620 cell line

The right section of Figure 10 depicts the protein expression patterns within the SW620 cell line following PFOA exposure, where a diminished expression of SMAD4 is noted, with a further decline as PFOA concentration increases. Similarly, the right section of Figure 11 illustrates the protein expression in the SW620 cell line after treatment with Gen-X, where SMAD4 is also found to be expressed at reduced levels.

The left panels of Figure 10 also demonstrate the gene expression differences in SW620 cell line after PFOA treatment. The results showed that a component of the TGF- $\beta$  signaling pathway, the TGF $\beta$ <sub>1</sub> gene, exhibited a significant increase in expression in PFOA-treated SW620 cells at IC<sub>50</sub> concentrations ( $p < 0.001$ ). However, the expression changes of TGF $\beta$ <sub>2</sub> and TGF $\beta$ <sub>3</sub> were not significant. SMAD family genes also showed different degrees of expression changes under the influence of PFOA. In particular, the expression levels of SMAD1, SMAD2 and SMAD4 were significantly increased in the IC<sub>50</sub> group ( $p < 0.001$ ), suggesting that the TGF- $\beta$  signaling pathway may play an important role in PFOA-mediated cellular effects. In addition, the expression of SMAD2 was also increased in the IC<sub>50</sub>-treated group, although this change did not show significance. In addition, the expression of p53, ATM, ATR, and the ribosomal protein genes RPL5 and RPL11 were all significantly increased in the IC<sub>50</sub> group, although this change was less significant in the  $\frac{1}{2}$  IC<sub>50</sub> group.

In the Gen-X treatment group (Fig. 11), the expression of target genes showed an overall decreasing trend. Within the TGF- $\beta$  family, there was a significant decreasing trend in TGF $\beta$ <sub>1</sub> ( $p < 0.001$ ), however, the expression of TGF $\beta$ <sub>2</sub> and TGF $\beta$ <sub>3</sub> increased but

did not show significance. The expression of SMAD family members was also significantly affected by Gen-X treatment. Specifically, the expression levels of SMAD1 and SMAD3 were significantly reduced in the IC<sub>50</sub> group (p < 0.001). SMAD2 exhibited decreased expression in both the 1/2 IC<sub>50</sub> and IC<sub>50</sub> groups (p < 0.01), whereas the expression of SMAD4 was significantly reduced in the 1/2 IC<sub>50</sub> group (p < 0.001). In addition, the expression of p53, ATM, ATR, and the ribosomal protein gene RPL5 were all significantly decreased in IC<sub>50</sub> group.

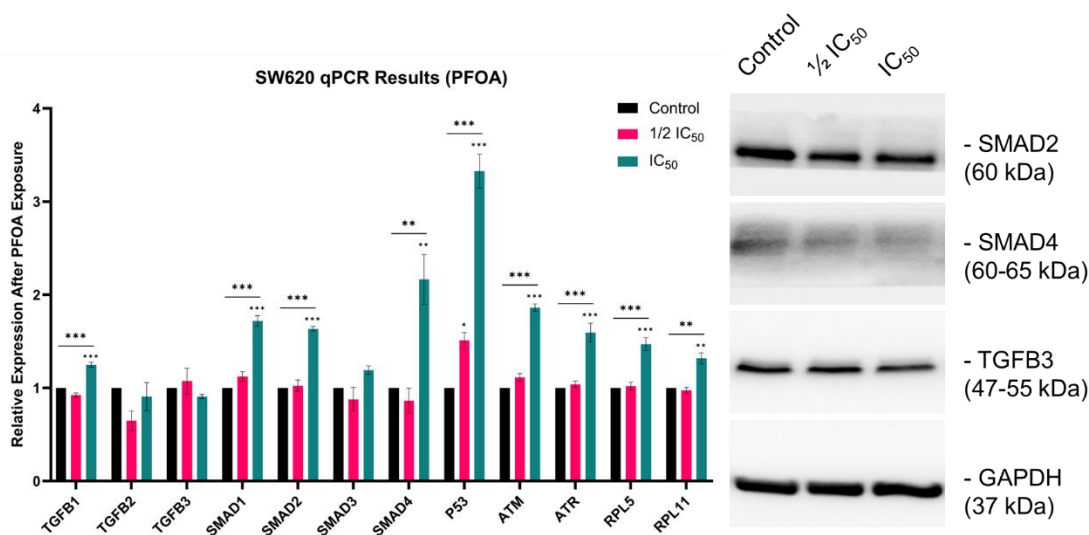


**Figure 10: Altered gene expression (left) and protein expression (right) in SW620 cells following exposure to PFOA.** SW620 cells were either mock-treated, or treated with PFOA with concentration of 1/2 IC<sub>50</sub>, IC<sub>50</sub> for 48 h, and then the relative mRNA levels were determined by RT-PCR. Data shown are mean ± SD of three independent experiments. \*, p < 0.05; \*\*, p < 0.01, \*\*\* p < 0.001. The lanes of each plot on the right panel represent, from left to right, the Control, the 1/2 IC<sub>50</sub> concentration target compound, and the IC<sub>50</sub> concentration target compound, respectively.

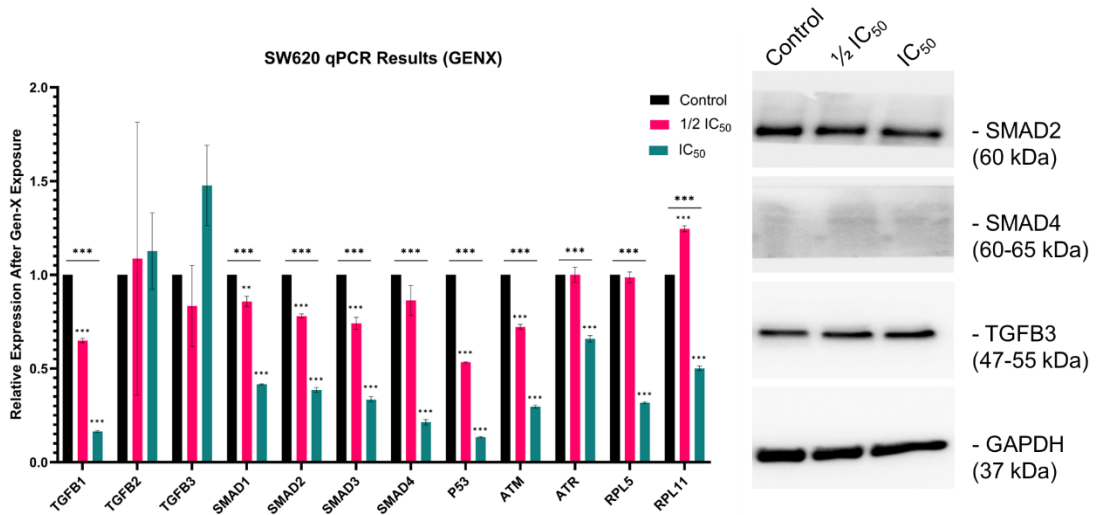


**Figure 11: Altered gene expression (left) and protein expression (right) in SW620 cells following exposure to Gen-X.** SW620 cells were either mock-treated, or treated with Gen-X with concentration of 1/2 IC<sub>50</sub>, IC<sub>50</sub> for 48 h, and then the relative mRNA levels were determined by RT-PCR. Data shown are mean ± SD of three independent experiments. \*, p < 0.05; \*\*, p < 0.01, \*\*\* p < 0.001. The lanes of each plot on the right panel represent, from left to right, the Control, the 1/2 IC<sub>50</sub> concentration target compound, and the IC<sub>50</sub> concentration target compound, respectively.

## Chapter 4: Discussion and Conclusion

### 4. Discussion and Conclusion

#### 4.1. Assessment of PFOA and Gen-X toxicity to cancer cells

This study systematically evaluated the cytotoxic effects of perfluorooctanoic acid (PFOA) and Gen-X on four different human cancer cell lines (A375, SN12C, HEPG2, SW620). By CCK-8 assay, this study examined the cellular activity of these cells under different concentrations of PFOA and Gen-X exposure for 48 h. The semi-inhibitory concentration ( $IC_{50}$ ) of each cell line was calculated by nonlinear regression analysis. In the A375 cell line, a high sensitivity to PFOA was observed, with an  $IC_{50}$  value of 213.2  $\mu$ M. In contrast, the A375 cell line showed a higher resistance to Gen-X, with an  $IC_{50}$  value of up to 1,555  $\mu$ M. This suggests that PFOA and Gen-X may affect the survival of A375 cells through different mechanisms or different intracellular targets (Charazac et al., 2022). The SN12C cell line showed strong resistance to PFOA with an  $IC_{50}$  of 616.3  $\mu$ M, while this cell line was even more resilient under Gen-X exposure, with an  $IC_{50}$  of 5048  $\mu$ M. In addition, it was observed that SN12C tended to proliferate under exposure to lower concentrations of Gen-X (<1000  $\mu$ M), and this remarkable resistance may be related to the renal cells' metabolic capacity and detoxification mechanism (Dong et al., 2023). The SW620 cell line showed moderate sensitivity to PFOA with an  $IC_{50}$  of 271.2  $\mu$ M. For Gen-X, SW620 also showed moderate resistance, with an  $IC_{50}$  of 2126  $\mu$ M. The HepG2 cell line showed lower sensitivity to PFOA, with an  $IC_{50}$  of 527.9  $\mu$ M, and further increased resistance to Gen-X, with an  $IC_{50}$  of 2377  $\mu$ M.

These results suggest that PFOA and Gen-X exhibit different cytotoxic properties in different cancer cell lines, which may reflect their different mechanisms of action at the molecular level, as well as the different response mechanisms of different cell lines to PFOA and Gen-X exposure (Zane & Schultz, 2020). In particular, the differential tolerance to PFOA and Gen-X may reveal differences in cell-specific metabolic and detoxification pathways. These findings are crucial for further understanding the mechanism of action of these compounds at the cellular level.

#### **4.1.1. Protein expression assessment**

In this study, the expression levels of GAPDH showed a high degree of consistency across all experimental groups, ensuring the accuracy of comparability between samples. GAPDH, a multifunctional enzyme crucial for processes including glycolysis, DNA repair, and cellular signaling, ensures accurate and reliable protein expression data (Cheung et al., 2014; Moein et al., 2017). The stability of GAPDH expression established a baseline for evaluating PFOA and Gen-X's effects on specific protein expressions in cancer cells, providing insights into their impact on cellular mechanisms such as survival, proliferation, and apoptosis.

The H2A.X protein is a member of the histone family, and its phosphorylated form ( $\gamma$ -H2A.X) is an early marker of almost any kind of DNA damage in cells (Suberbielle et al., 2013). In the present study, it was observed that the level of modification of  $\gamma$ -H2A.X increased with increasing drug concentration upon exposure to PFOA and Gen-X in different cell lines. In particular, in the A375 cell line,  $\gamma$ -H2A.X was observed in

all groups but did not show a significant trend. In SN12C cell line, on the other hand,  $\gamma$ -H2A.X was not observed in the control group, while its abundance gradually increased with increasing exposure to PFOA and Gen-X. The abundance trend in HepG2 cell line was similar to that of SN12C. In the SW620 cell line,  $\gamma$ -H2A.X abundance in the Gen-X exposure group increased with increasing concentration, while no significant  $\gamma$ -H2A.X abundance was observed in the PFOA group. These results suggest that PFOA and Gen-X may cause intracellular DNA damage, especially in the A375 and SN12C cell lines. Increased abundance of  $\gamma$ -H2A.X may reflect a DNA damage response initiated by cells to maintain genome integrity (Mah et al., 2010). The differences in  $\gamma$ -H2A.X abundance patterns observed in different cell lines may be related to cell type-specific DNA repair capabilities. For example, the renal cancer cell line SN12C exhibited a proliferative tendency under low concentrations of Gen-X exposure, which may be related to its unique mechanism in DNA damage repair and cell cycle regulation. In addition, the increased expression of  $\gamma$ -H2A.X may also be associated with the apoptotic process. Previous studies have shown that the formation of  $\gamma$ -H2A.X is closely associated with apoptosis induction, and particularly the formation of large numbers of  $\gamma$ -H2A.X spots in the nucleus is associated with the initiation of programmed cell death (Ba & Yu, 2022). Therefore, the increased  $\gamma$ -H2A.X abundance observed in this study may reflect the mechanism of apoptosis changed susceptibility of these cell lines to DNA damage induced by PFOA and Gen-X.

#### **4.1.2.PFOA and Gen-X induce significant changes in gene expression in**

#### **four kinds of human cancer cell lines**

The present study analyzed in detail the changes in the expression of several key proteins (e.g., SMAD4, TGF $\beta$ 3, SMAD2) in different cancer cell lines (A375, SN12C, HepG2, SW620) under PFOA and Gen-X treatments. These changes revealed the potential effects of different compounds on cell signaling pathways.

##### **4.1.2.1. Response of the A375 cell line**

In the A375 skin melanoma cell line, PFOA and Gen-X treatments caused significant changes in the TGF $\beta$ 3 and SMAD2 genes at the mRNA level. These changes suggest that the TGF- $\beta$  signaling pathway is activated in response to PFOA and Gen-X exposure. At the protein level, a significant increase in SMAD4 expression was observed in the PFOA-treated group, which was consistent with the changes at the transcriptional level. SMAD4 is a central component of the TGF- $\beta$  signaling pathway, and its upregulation may be a direct response to the activation of the TGF- $\beta$  signaling pathway (Zhao et al., 2018). In previous studies, SMAD4 is usually mutated or deleted in a manner that leads to cancer development and metastasis. For example, in pancreatic ductal adenocarcinoma (PDAC), deletion of SMAD4 enhances glycolysis and invasive tumor behavior by upregulating PGK1 (Liang et al., 2020). The significant increase in SMAD4 expression observed in A375 cells is probably a cellular response to DNA damage caused by PFOA. Studies have shown that the TGF- $\beta$  signaling pathway plays a complex and two-fold role in the development and progression of cancer. On the one hand, it plays an inhibitory role in the early stages of cancer; on the other hand, the

pathway may promote tumor proliferation and metastasis after the tumor has progressed to a certain stage (Ciardiello et al., 2020). It has been found that a compound called mono(2-ethylhexyl) phthalate (MEHP) significantly increased the migration and invasive ability of A375 cells. MEHP can increase the expression of TGF- $\beta$  and promoted the activation of Smad signaling and the up-regulation of Snail in melanoma cells through the up-regulation of TGF- $\beta$ , which resulted in an increase in the migration and invasive ability of cancer cells (Fan et al., 2020). This found is similar to the effect caused by PFOA on the TGF- $\beta$  pathway in A375 cells found in this study.

It is interesting to note that p53 gene expression was significantly down-regulated at Gen-X IC<sub>50</sub> concentrations and was not detected to be significantly changed by PFOA exposure. The tumor suppressor protein p53 plays a crucial role in maintaining genomic stability and preventing tumor formation. It functions in pluripotent stem cells to maintain genomic stability by inducing cell cycle arrest, apoptosis, and senescence in response to DNA damage or oncogenic stress (Fu et al., 2020). The expression of p53 was down-regulated or unchanged under PFOA and Gen-X exposure, suggesting that these compounds may have impaired the cell's DNA damage response mechanisms. This situation may lead to a failure to repair DNA damage appropriately, increasing the risk of cell mutation and cancer development. Accordingly, a significant increase in ATM/ATR expression in A375 cells can be found. ATM and ATR are key components of the DNA damage response (DDR), which activate cell cycle checkpoints and DNA repair mechanisms by sensing DNA damage such as double-strand breaks and replication stress (Maréchal & Zou, 2013). In the presence of impaired p53 function,

upregulation of ATM/ATR may be a compensatory mechanism that attempts to maintain DNA integrity by activating other pathways.

In addition, a significant increase in RPL5 and RPL11 expression in A375 cells was also observed in the PFOA-treated group. RPL5 and RPL11 play a critical role in the regulation of the tumor suppressor protein p53 and are involved in the cellular response to ribosomal stress. These ribosomal proteins inhibit Hdm2 in an interdependent manner, stabilize p53, and activate new G2/M checkpoints in response to impaired ribosome biogenesis (Donati et al., 2013; Fumagalli et al., 2012). Moreover, RPL5 and RPL11 are positive regulators of p53 that act as tumor suppressors, upregulating p53 and preventing tumorigenesis by binding to and inhibiting MDM2 ubiquitin ligase (Li et al., 2022). However, p53 did not show a tendency to be upregulated, which further suggests that the stress response mechanisms in the cell are altered or impaired.

PFOA and Gen-X exposure induced several biological changes in A375 cutaneous melanoma cells that may disrupt cellular stress response mechanisms and increase the risk of cancer development. These compounds activated the TGF- $\beta$  signaling pathway and led to down-regulation or no change in the expression of the p53 gene, which is an important tumor suppressor. Furthermore, despite increased expression of ATM/ATR and RPL5/RPL11, there was no concomitant upregulation of p53, suggesting that the cellular response to DNA damage may be compromised. Thus, these findings imply that PFOA and Gen-X may negatively impact cellular health and promote cancer development.

#### 4.1.2.2. Response of the SN12C cell line

The SN12C cell line is derived from human kidney cancer cells and is characterized by high tumorigenicity and weak metastasis (Coughlin et al., 2013). Studies have shown that kidney cells may exhibit unique sensitivities to certain compounds due to their filtering and detoxification role in the body (Hosohata, 2016; Masereeuw, 2022). In this study, PFOA and Gen-X treatments caused significant changes in the expression of TGF- $\beta$  family genes and SMAD family genes in SN12C cells. Especially in the PFOA-treated group, the expression of both TGF- $\beta$  family genes and SMAD family genes was significantly down-regulated, which may be related to the higher resistance of SN12C cells to PFOA observed in the CCK-8 experiment of present study. A study found that after down-regulation of TGF- $\beta$  and SMAD3 signaling by a specific inhibitor (SIS3), renal fibrosis, apoptosis, and inflammation were reduced (Ji et al., 2018). This finding is similar to that observed in the present study, where a similar stress response mechanism may exist in SN12C cells. Under the chemical stress of PFOA, SN12C cells showed high resistance to PFOA by downregulating TGF- $\beta$  and SMAD signaling pathways and reducing apoptosis.

In the Gen-X exposed group, a completely different expression trend was observed. TGF- $\beta$  signaling was not up-regulated, but the SMAD signaling pathway showed a trend of up-regulation. In addition, distinct from the A375 cell line, there was a significant increase in the expression of p53, and other genes associated with DNA repair and cancer suppression, such as ATM/ATR, and PRL5/RPL11, were significantly up-regulated. This indicates that the cellular stress response mechanism of SN12C did

not experience obvious changes under Gen-X exposure, which explains the extremely high tolerance ( $IC_{50}$ : 5048  $\mu$ M) of SN12C to Gen-X. Notably, in the Gen-X-exposed group, it can be observed that the protein expression trend of SMAD4 is not consistent with the mRNA expression trend. Although no similar situation in renal cancer cells has been reported in the literature in previous studies, there are still hypotheses in the literature about the inconsistent mRNA and protein expression of SMAD4. It has been suggested that the discrepancy between SMAD4 mRNA and protein expression may be related to microRNA. In this study, after studying porcine follicular granulosa cells, microRNA-26b (miR-26b) was found to target the 3'-untranslated region of the SMAD4 gene, resulting in suppression of SMAD4 mRNA and protein levels (J. Liu et al., 2014). In addition, it was also found that in granulocyte precursors, miR-130a targets Smad4 mRNA, leading to a decrease in Smad4 protein synthesis without affecting mRNA levels (Häger et al., 2011). These findings suggest that post-transcriptional regulation of microRNAs can lead to a mismatch between mRNA and protein expression levels. The response of SN12C cells to PFOA and Gen-X provides preliminary evidence that these two chemicals are potentially damaging to DNA and alter the cellular DNA damage response and cancer suppression mechanisms by affecting the TGF- $\beta$  signaling pathway and the synthesis of related proteins. In addition, the inconsistent results of mRNA and protein expression after Gen-X exposure suggest that Gen-X may have epigenetic toxicity.

#### **4.1.2.3. Response of the HepG2 cell line**

HepG2 cell line, a human hepatocellular carcinoma cell model commonly used in cytotoxicology and cancer research. Since the liver plays a central role in the body's metabolism and detoxification (Lao et al., 2021; Schwen et al., 2015), the response of HepG2 cells to PFOA and Gen-X may reflect liver cell-specific processing mechanisms for these compounds. The toxicity of PFOA and Gen-X to HepG2 cells has been discussed in several papers. It has been shown that PFOA at concentrations of 50-400  $\mu\text{M}$  causes DNA strand breaks and micronuclei in HepG2 cells in a dose-dependent manner (Yao & Zhong, 2005). A recent study found that PFOA and Gen-X significantly affect cell cycle genes, Ten-Eleven Translocated Methylcytosine Dioxygenases (TETs) and important lipid metabolism genes in HepG2 cells (Wen et al., 2020). In this study, significant abundance of  $\gamma\text{-H2A.X}$  was observed in HepG2 cells treated with PFOA and Gen-X  $\text{IC}_{50}$  concentrations, indicating cellular activation of DNA damage response mechanisms. p53, ATM/ATM, and RPL5/RPL11 also showed significant up-regulation to varying degrees, further validating the presence of DNA strand damage within the cells. These response results observed in HepG2 cells are consistent with the findings in previous studies demonstrating the genotoxicity of PFOA and Gen-X (Wen et al., 2020; Yao & Zhong, 2005).

In terms of the TGF- $\beta$  signaling pathway, the present study observed that TGF- $\beta_1$  was overexpressed after treatment with PFOA and Gen-X. The TGF- $\beta$  signaling pathway has important contributions in the development of liver diseases, especially liver fibrosis and hepatocellular carcinoma formation (Fabregat et al., 2016). In addition, it has been found that high levels of TGF- $\beta_1$  can activate both SMAD and Erk dominant

pathways to induce hepatocellular carcinoma and cholangiocarcinoma (C. Yan et al., 2017). The hyperactivation of TGF- $\beta_1$  reflects the potential promotional effect of PFOA and Gen-X on hepatocellular carcinoma cells.

#### **4.1.2.4. Response of the SW620 cell line**

The SW620 cell line, derived from human colon cancer, is an important model for studying colon cancer cell biology and drug response. In SW620 cells, PFOA and Gen-X exposure resulted in changes in TGF- $\beta$  and SMAD family gene expression. In the PFOA-exposed group, both the TGF- $\beta$  signaling pathway and the SMAD signaling pathway were significantly up-regulated, but this change was only observed in the IC<sub>50</sub>-exposed group and the up-regulation was not significant. In the  $\frac{1}{2}$  IC<sub>50</sub>-exposed group, no significant expression change from the control group was observed. This suggests that the results observed from the experiment may be a metabolic regulation and stress response made by SW620 cells under high chemical stress. In terms of genotoxicity, from the expression results of  $\gamma$ -H2A.X only a very small amount of protein expression could be observed in the IC<sub>50</sub>-treated group, but the expression of p53, ATM/ATR, and RPL5/RPL11 were all significantly elevated. These results suggest that the high concentration of PFOA caused damage to the DNA of SW620.

It was interesting to note that SMAD4 was significantly upregulated in mRNA expression, but very low SMAD4 protein expression could be found in SW620 cells in the protein expression results, this phenomenon may make the condition of colon cancer patients worse. Studies have shown that SMAD4 inactivation promotes malignancy and

drug resistance in colon cancer, and that the TGF $\beta$ -induced MEK-Erk and p38-MAPK (mitogen-activated protein kinase) auxiliary pathways are hyperactivated in SMAD4-deficient cells. Activation of these pathways is associated with increased expression of VEGF, which promotes tumor angiogenesis. VEGF is a major pro-angiogenic factor critical for tumor growth and metastasis (Papageorgis et al., 2011). In addition, many studies have reported that decreased SMAD4 expression is associated with poor survival in colon cancer patients (P. Yan et al., 2016), poor clinical outcomes (Freeman et al., 2012), and colon cancer progression and metastasis (Voorneveld et al., 2014). From this finding, it is reasonable to hypothesize that colon cancer patients who are chronically exposed to PFOA or Gen-X may have reduced SMAD4 expression in their body's cancer cells, leading to metastasis and progression.

#### **4.1.3. Strength and limitations**

The present study demonstrates several strengths in exploring the effects of PFOA and Gen-X on human cancer cell lines. First, a major strength of this study is its multi-cell line approach. By involving a variety of cancer cell lines such as A375 (melanoma), SN12C (renal cancer), HepG2 (hepatocellular carcinoma), and SW620 (colon cancer), the study provides a broad perspective on the effects of PFOA and Gen-X. This diversity allowed the study to capture subtle differences in the response of different types of cancer cells to these compounds, thereby revealing possible cell-specific mechanisms of action. This is critical to understanding the possible unique roles and effects of these compounds in different cancer types. Second, this study employed

multiple experimental techniques, including CCK-8 cytotoxicity assessment, western blot and RT-PCR analyses, and this integrated approach allowed for a more comprehensive and in-depth conclusion of the study. This approach not only allowed for the assessment of the effects of PFOA and Gen-X on cell survival, but also allowed for an in-depth exploration of how these compounds alter the expression of important proteins and genes within the cell. This provides critical data for a deeper understanding of their molecular mechanisms of action. Finally, the importance of this study is its investigation of compounds of current environmental concern, PFOA and Gen-X. With the widespread use of these compounds in the environment and in industrial products, it has become particularly important to understand their potential effects on human health. The findings of this study help the public and the scientific community to better understand the biological effects of these environmental contaminants and provide a scientific basis for future environmental safety policies and health risk assessments.

While the present study has made progress in exploring the effects of PFOA and Gen-X on a variety of cancer cell lines, some limitations still exist that should be considered when planning future studies. First, this study depended primarily on in vitro cellular experiments without in vivo experimental validation. While in vitro experiments provide convenience and control for preliminary explorations, they usually cannot fully mimic the complex environment and interactions in organisms (H.-H. Hu et al., 2018). This is especially true for chemicals such as PFOA and Gen-X, which may exhibit different kinetic properties and mechanisms of action in organisms. Therefore, the results of this study need to be further validated in in vivo models to ensure the

biological relevance and applicability of the conclusions. Second, this study lacked temporal and dose diversity in some respects. Although the study examined the short-term effects of PFOA and Gen-X on cells, long-term exposures may have different or more severe effects, particularly in terms of cancer progression and cellular adaptation. In addition, studies have focused on specific concentration ranges and may have failed to reveal cellular responses at lower or higher concentrations, which limits the scope for a comprehensive understanding of the toxic properties of PFOA and Gen-X. Furthermore, there was a possible flaw in the primer design of this study. In the RT-PCR results of A375 and HepG2, the expression signal of TGF $\beta$ 2 could not be observed, resulting in missing data, and the primer design of TGF $\beta$ 2 corresponding to cell lines should be taken into account in future studies. Finally, this study is limited in directly demonstrating the specific mechanisms of action of PFOA and Gen-X. Although changes in signaling pathways were observed, it failed to directly link these changes to specific molecular actions of PFOA and Gen-X. This mechanistic uncertainty may affect the understanding of the nature of the compounds' actions and limit the ability to develop targeted intervention strategies at the molecular level.

## **4.2. Conclusion**

In conclusion, the present study provides insights into the effects of PFOA and Gen-X on different human cancer cell lines (A375, SN12C, HepG2, SW620) and reveals the mechanism of action of these environmental pollutants at the cellular level. It was found that these compounds exhibited unique cytotoxic effects in different cancer cell lines

and may affect cell survival and proliferation by modulating specific signaling pathways such as TGF- $\beta$ /SMAD. These results provide an important scientific basis for understanding the potential effects of PFOA and Gen-X in living organisms.

In future studies, several key directions need to be focused on to further deepen the understanding of the mechanisms of action of PFOA and Gen-X. First, *in vivo* experimental validation is essential and will help confirm the biological relevance of *in vitro* results and reveal the kinetics and mechanisms of action of these compounds throughout the organism. Second, studies of long-term exposure effects will reveal the long-term impact of these compounds on cellular behavior, particularly in terms of tumor progression and cellular adaptation. In addition, studies considering different concentrations and time points will help to comprehensively assess the cytotoxic properties of these compounds. Finally, an in-depth exploration of how the compounds specifically modulate signaling pathways, and how they affect the cell cycle, apoptosis, and DNA damage response, will be critical for the development of preventive and therapeutic strategies.

## Appendix A: List of chemicals

Chemicals	Brand	Catalog Number
Perfluorooctanoic acid	Aladdin	P106681
Perfluoro(2-methyl-3-oxahexanoic) acid	Aladdin	P302398
Dulbecco's modified eagle medium (DMEM)	Gibco	C11995500BT
Fetal bovine serum (FBS)	Gibco	A5669701
Penicillin-Streptomycin (P/S)	Gibco	15070063
Trypsin-EDTA (0.25%) with phenol red	Gibco	25200056
Dimethyl sulfoxide (DMSO)	Solarbio	D8371
1M Tris pH 6.8	Quayad	QYR011
1M Tris pH 8.8	Quayad	QYR032
Sodium Dodecyl Sulfate (SDS)	BioFroxx	3250
Bovine Serum Albumin (BSA)	BioFroxx	4240
Tris-base	BioFroxx	1115
Glycine	BioFroxx	1275
Ammonium Persulfate (APS)	MACKIIN	A6295
N,N,N',N'-Tetramethylethylenediamine	MACKIIN	T6023
Tween 20	VE TEC	V900548
Methanol	Adamas	75851G
Chloroform	Adamas	75915R
DEPC water	Adamas life	G8010
RNase-free ddH <sub>2</sub> O	Adamas life	G8051
PageRuler™ Prestained protein MW standard, 10 to 180 kDa	Thermo Fisher Scientific	26616
ECL WB substrate	Tanon	180-501
Trizol	Sigma-Aldrich Corporation	T9424
Phosphate Buffered Saline (PBS 1X)	Meilunbio	MA0015-1
HiScript II 1st Strand cDNA Synthesis Kit	Vazyme	R211-02
ChamQ Universal SYBR qPCR Master Mix	Vazyme	Q711-02
Enhanced Cell Counting Kit-8	Beyotime	C0042
30% Acr-Bis (29:1)	Beyotime	ST003
GAPDH Mouse mAb	Cell Signaling Technology	97166

Phospho-Histone H2A.X Rabbit mAb	Cell Signaling Technology	9718
Smad2 Rabbit Monoclonal Antibody	Beyotime	AF1300
SMAD4 Rabbit mAb	Abcam	ab40759
TGFβ3 Rabbit mAb	Abcam	ab308300

## Appendix B: Gel and buffer recipes

### B.1: Separation Gel

Gradients	Volume(mL)			
10% gel	10.0	20.0	30.0	40.0
ddH <sub>2</sub> O	2.7	5.3	8.0	10.6
30%Acr-Bis(29:1)	3.3	6.7	10.0	12.4
1 M Tris, pH8.8	3.8	7.6	11.4	15.2
10%SDS	0.1	0.2	0.3	0.4
10%APS	0.1	0.2	0.3	0.4
TEMED	0.004	0.008	0.012	0.016

Gradients	Volume(mL)			
15% gel	10.0	20.0	30.0	40.0
ddH <sub>2</sub> O	1.0	2.0	3.0	4.0
30%Acr-Bis(29:1)	5.0	10.0	10.0	12.4
1 M Tris, pH8.8	3.8	7.6	11.4	15.2
10%SDS	0.1	0.2	0.3	0.4
10%APS	0.1	0.2	0.3	0.4
TEMED	0.004	0.008	0.012	0.016

### B.2: Stacking Gel

Gradients	Volume(mL)			
15% gel	4.0	6.0	8.0	10.0
ddH <sub>2</sub> O	2.7	4.1	5.5	6.8
30%Acr-Bis(29:1)	0.67	1.00	1.30	1.70
1 M Tris, pH8.8	0.50	0.75	1.00	1.25
10%SDS	0.04	0.06	0.08	0.10
10%APS	0.04	0.06	0.08	0.10
TEMED	0.004	0.006	0.008	0.010

### B.3: Tris-Glycine running buffer

Tris base	3.024 g
Glycine	14.4 g
SDS	1 g
ddH <sub>2</sub> O	1000mL

### B.4: 10x Transferring buffer

Tris base	30.2 g
Glycine	144 g
ddH <sub>2</sub> O	1L

**B.5: 1x Transferring buffer**

10x Transferring buffer	100 mL
Methanol	200 mL
ddH <sub>2</sub> O	700 mL

**B.6: 10xTBS (Tris-buffered saline)**

NaCl	160 g
Tris base	48 g
ddH <sub>2</sub> O	2000mL

**B.7: TBST (Tris-buffered saline with Tween 20)**

10xTBS	100mL
Tween 20	1mL
ddH <sub>2</sub> O	900mL

## Appendix C: RT-PCR Primers

Gene	Primer sequence	Product size
ATM	F: GAGCAGAGTCTTGCCCTGAG	20
	R: TTTAGGCTGGGATTGTTCGCT	21
ATR	F: CCAGTGAAAGGGCATTCCAA	20
	R: GAACATGGGTCTTGGCCTTTT	21
TGF $\beta$ <sub>1</sub>	F: GGAAATTGAGGGCTTTCGCC	20
	R: CCGGTAGTGAACCCGTTGAT	20
TGF $\beta$ <sub>2</sub>	F: CGAGAGGAGCGACGAAGAGT	20
	R: ACAACTGGGCAGACAGTTTCG	21
TGF $\beta$ <sub>3</sub>	F: GGAAAACACCGAGTCGGAATAC	22
	R: GCGGAAAACCTTGGAGGTAAT	21
SMAD1	F: CCGATGGACACAAACATGATGGC	23
	R: AAGCAACCGCCTGAACATCTCC	22
SMAD2	F: GTCCATCTTGCCATTCACG	19
	R: CTCAAGCTCATCTAATCGTCCTG	23
SMAD3	F: AAGGACGAGGTCTGCGTGAATC	22
	R: CCAACACAGGAGGTAGAACTGGTG	24
SMAD4	F: TCCTGTGGCTTCCACAAGTCAG	22
	R: GCCCTGATGCTATCTGCAACAGTC	24
RPL5	F: CAACACACCCAAATACAGGATG	22
	R: CGGGCATAAGCAATCTGACAA	21
RPL11	F: GTCCACTGCACAGTTCGAGG	20
	R: AACTCATACTCCCGCACCTTT	21
p53	F: CAGCACATGACGGAGGTTGT	20
	R: TCATCCAAATACTCCACACGC	21
GAPDH	F: ACAACTTTGGTATCGTGGAAGG	22
	R: GCCATCACGCCACAGTTTC	19

## Reference list

- Abudayyak, M., Öztaş, E., & Özhan, G. (2021). Determination of Perfluorooctanoic Acid Toxicity in a Human Hepatocarcinoma Cell Line. *Journal of Health & Pollution*, *11*(31), 210909. <https://doi.org/10.5696/2156-9614-11.31.210909>
- Ba, S., & Yu, M. (2022). Ultrasound-stimulated microbubbles enhances radiosensitivity of ovarian cancer. *Acta Radiologica*, *63*(10), 1433–1440. <https://doi.org/10.1177/02841851211038808>
- Bartell, S. M., & Vieira, V. M. (2021). Critical review on PFOA, kidney cancer, and testicular cancer. *Journal of the Air & Waste Management Association (1995)*, *71*(6), 663–679. <https://doi.org/10.1080/10962247.2021.1909668>
- Blake, B. E., Cope, H. A., Hall, S. M., Keys, R. D., Mahler, B. W., McCord, J., Scott, B., Stapleton, H. M., Strynar, M. J., Elmore, S. A., & Fenton, S. E. (2020). Evaluation of Maternal, Embryo, and Placental Effects in CD-1 Mice following Gestational Exposure to Perfluorooctanoic Acid (PFOA) or Hexafluoropropylene Oxide Dimer Acid (HFPO-DA or GenX). *Environmental Health Perspectives*, *128*(2), 027006. <https://doi.org/10.1289/EHP6233>
- Buck, R. C., Franklin, J., Berger, U., Conder, J. M., Cousins, I. T., de Voogt, P., Jensen, A. A., Kannan, K., Mabury, S. A., & van Leeuwen, S. P. J. (2011). Perfluoroalkyl and polyfluoroalkyl substances in the environment: Terminology, classification, and origins. *Integrated Environmental Assessment and Management*, *7*(4), 513–541. <https://doi.org/10.1002/ieam.258>
- Charazac, A., Hinault, C., Bost, F., Clavel, S., & Chevalier, N. (2019). Low doses of persistent organic pollutants (PFOA and PCB153) increase the tumor aggressiveness of hormone-dependent cancer cells. *Endocrine Abstracts*, *63*. <https://doi.org/10.1530/endoabs.63.P999>
- Charazac, A., Hinault, C., Dolfi, B., Hautier, S., Decondé Le Butor, C., Bost, F., & Chevalier, N. (2022). Low Doses of PFOA Promote Prostate and Breast Cancer Cells Growth through Different Pathways. *International Journal of Molecular Sciences*, *23*(14), Article 14. <https://doi.org/10.3390/ijms23147900>
- Cheung, J. L. K., Cheung, T. H., Yu, M. Y., Yeung, A. C. M., & Chan, P. K. S. (2014). Selection of Referent Transcript for Normalization of Gene Expression in Cervical Cytology Samples. *Applied Immunohistochemistry & Molecular Morphology*, *22*(2), 153. <https://doi.org/10.1097/PDM.0b013e318299cc14>
- Ciardello, D., Elez, E., Taberner, J., & Seoane, J. (2020). Clinical development of therapies targeting TGFβ: Current knowledge and future perspectives. *Annals of Oncology*, *31*(10), 1336–1349. <https://doi.org/10.1016/j.annonc.2020.07.009>
- Conley, J. M., Lambright, C. S., Evans, N., Strynar, M. J., McCord, J., McIntyre, B. S., Travlos, G.

S., Cardon, M. C., Medlock, -Kakaley Elizabeth, Hartig, P. C., Wilson, V. S., & Gray, L. E. (2019). Adverse Maternal, Fetal, and Postnatal Effects of Hexafluoropropylene Oxide Dimer Acid (GenX) from Oral Gestational Exposure in Sprague-Dawley Rats. *Environmental Health Perspectives*, 127(3), 037008. <https://doi.org/10.1289/EHP4372>

Coperchini, F., Awwad, O., Rotondi, M., Santini, F., Imbriani, M., & Chiovato, L. (2017). Thyroid disruption by perfluorooctane sulfonate (PFOS) and perfluorooctanoate (PFOA). *Journal of Endocrinological Investigation*, 40(2), 105–121. <https://doi.org/10.1007/s40618-016-0572-z>

Coperchini, F., Croce, L., Ricci, G., Magri, F., Rotondi, M., Imbriani, M., & Chiovato, L. (2020). Thyroid Disrupting Effects of Old and New Generation PFAS. *Frontiers in Endocrinology*, 11, 612320. <https://doi.org/10.3389/fendo.2020.612320>

Coughlin, M. F., Bielenberg, D. R., Lenormand, G., Marinkovic, M., Waghorne, C. G., Zetter, B. R., & Fredberg, J. J. (2013). Cytoskeletal stiffness, friction, and fluidity of cancer cell lines with different metastatic potential. *Clinical & Experimental Metastasis*, 30(3), 237–250. <https://doi.org/10.1007/s10585-012-9531-z>

De Silva, A. O., Armitage, J. M., Bruton, T. A., Dassuncao, C., Heiger-Bernays, W., Hu, X. C., Kärman, A., Kelly, B., Ng, C., Robuck, A., Sun, M., Webster, T. F., & Sunderland, E. M. (2021). PFAS Exposure Pathways for Humans and Wildlife: A Synthesis of Current Knowledge and Key Gaps in Understanding. *Environmental Toxicology and Chemistry*, 40(3), 631–657. <https://doi.org/10.1002/etc.4935>

Donati, G., Peddigari, S., Mercer, C. A., & Thomas, G. (2013). 5S Ribosomal RNA Is an Essential Component of a Nascent Ribosomal Precursor Complex that Regulates the Hdm2-p53 Checkpoint. *Cell Reports*, 4(1), 87–98. <https://doi.org/10.1016/j.celrep.2013.05.045>

Dong, X.-Q., Chu, L.-K., Cao, X., Xiong, Q.-W., Mao, Y.-M., Chen, C.-H., Bi, Y.-L., Liu, J., & Yan, X.-M. (2023). Glutathione metabolism rewiring protects renal tubule cells against cisplatin-induced apoptosis and ferroptosis. *Redox Report*, 28(1), 2152607. <https://doi.org/10.1080/13510002.2022.2152607>

Eriksson, U., & Kärman, A. (2015). World-Wide Indoor Exposure to Polyfluoroalkyl Phosphate Esters (PAPs) and other PFASs in Household Dust. *Environmental Science & Technology*, 49(24), 14503–14511. <https://doi.org/10.1021/acs.est.5b00679>

Evich, M. G., Davis, M. J. B., McCord, J. P., Acrey, B., Awkerman, J. A., Knappe, D. R. U., Lindstrom, A. B., Speth, T. F., Tebes-Stevens, C., Strynar, M. J., Wang, Z., Weber, E. J., Henderson, W. M., & Washington, J. W. (2022). Per- and polyfluoroalkyl substances in the environment. *Science (New York, N.Y.)*, 375(6580), eabg9065. <https://doi.org/10.1126/science.abg9065>

Fabregat, I., Moreno-Càceres, J., Sánchez, A., Dooley, S., Dewidar, B., Giannelli, G., ten Dijke, P., & Consortium, the I.-L. (2016). TGF- $\beta$  signalling and liver disease. *The FEBS Journal*, 283(12),

2219–2232. <https://doi.org/10.1111/febs.13665>

Fan, P., Li, Z., Zuo, C., & Fang, M. (2020). Promotion effects of mono-2-ethylhexyl phthalate (MEHP) on migration and invasion of human melanoma cells via activation of TGF- $\beta$  signals. *Cell Biochemistry and Function*, 38(1), 38–46. <https://doi.org/10.1002/cbf.3447>

Freeman, T. J., Smith, J. J., Chen, X., Washington, M. K., Roland, J. T., Means, A. L., Eschrich, S. A., Yeatman, T. J., Deane, N. G., & Beauchamp, R. D. (2012). Smad4-Mediated Signaling Inhibits Intestinal Neoplasia by Inhibiting Expression of  $\beta$ -Catenin. *Gastroenterology*, 142(3), 562-571.e2. <https://doi.org/10.1053/j.gastro.2011.11.026>

Fu, X., Wu, S., Li, B., Xu, Y., & Liu, J. (2020). Functions of p53 in pluripotent stem cells. *Protein & Cell*, 11(1), 71–78. <https://doi.org/10.1007/s13238-019-00665-x>

Fumagalli, S., Ivanenkov, V. V., Teng, T., & Thomas, G. (2012). Suprainduction of p53 by disruption of 40S and 60S ribosome biogenesis leads to the activation of a novel G2/M checkpoint. *Genes & Development*, 26(10), 1028–1040. <https://doi.org/10.1101/gad.189951.112>

Gandhi, V., O'Brien, M. H., & Yadav, S. (2020). High-Quality and High-Yield RNA Extraction Method From Whole Human Saliva. *Biomarker Insights*, 15, 1177271920929705. <https://doi.org/10.1177/1177271920929705>

Gilliland, F. D., & Mandel, J. S. (1993). Mortality among employees of a perfluorooctanoic acid production plant. *Journal of Occupational Medicine.: Official Publication of the Industrial Medical Association*, 35(9), 950–954. <https://doi.org/10.1097/00043764-199309000-00020>

Gomis, M. I., Vestergren, R., Borg, D., & Cousins, I. T. (2018). Comparing the toxic potency in vivo of long-chain perfluoroalkyl acids and fluorinated alternatives. *Environment International*, 113, 1–9. <https://doi.org/10.1016/j.envint.2018.01.011>

Häger, M., Pedersen, C. C., Larsen, M. T., Andersen, M. K., Hother, C., Grønbæk, K., Jarmer, H., Borregaard, N., & Cowland, J. B. (2011). MicroRNA-130a-mediated down-regulation of Smad4 contributes to reduced sensitivity to TGF- $\beta$ 1 stimulation in granulocytic precursors. *Blood*, 118(25), 6649–6659. <https://doi.org/10.1182/blood-2011-03-339978>

Hosohata, K. (2016). Role of Oxidative Stress in Drug-Induced Kidney Injury. *International Journal of Molecular Sciences*, 17(11), Article 11. <https://doi.org/10.3390/ijms17111826>

Hu, H.-H., Chen, D.-Q., Wang, Y.-N., Feng, Y.-L., Cao, G., Vaziri, N. D., & Zhao, Y.-Y. (2018). New insights into TGF- $\beta$ /Smad signaling in tissue fibrosis. *Chemico-Biological Interactions*, 292, 76–83. <https://doi.org/10.1016/j.cbi.2018.07.008>

Hu, K., Fu, M., Wang, J., Luo, S., Barreto, M., Singh, R., Chowdhury, T., Li, M., Zhang, M., Guan, X., Xiao, J., & Hu, Q. (2020). HSV-2 Infection of Human Genital Epithelial Cells Upregulates TLR9

Expression Through the SP1/JNK Signaling Pathway. *Frontiers in Immunology*, 11. <https://www.frontiersin.org/articles/10.3389/fimmu.2020.00356>

Ji, X., Wang, H., Wu, Z., Zhong, X., Zhu, M., Zhang, Y., Tan, R., Liu, Y., Li, J., & Wang, L. (2018). Specific Inhibitor of Smad3 (SIS3) Attenuates Fibrosis, Apoptosis, and Inflammation in Unilateral Ureteral Obstruction Kidneys by Inhibition of Transforming Growth Factor  $\beta$  (TGF- $\beta$ )/Smad3 Signaling. *Medical Science Monitor*, 24, 1633–1641. <https://doi.org/10.12659/MSM.909236>

Jian, J.-M., Chen, D., Han, F.-J., Guo, Y., Zeng, L., Lu, X., & Wang, F. (2018). A short review on human exposure to and tissue distribution of per- and polyfluoroalkyl substances (PFASs). *Science of The Total Environment*, 636, 1058–1069. <https://doi.org/10.1016/j.scitotenv.2018.04.380>

Kwiatkowski, C. F., Andrews, D. Q., Birnbaum, L. S., Bruton, T. A., DeWitt, J. C., Knappe, D. R. U., Maffini, M. V., Miller, M. F., Pelch, K. E., Reade, A., Soehl, A., Trier, X., Venier, M., Wagner, C. C., Wang, Z., & Blum, A. (2020). Scientific Basis for Managing PFAS as a Chemical Class. *Environmental Science & Technology Letters*, 7(8), 532–543. <https://doi.org/10.1021/acs.estlett.0c00255>

Lao, Y., Li, Y., Wang, W., Ren, L., Qian, X., He, F., Chen, X., & Jiang, Y. (2021). *A Cytological Atlas of Human Liver Proteome from PROTEOME<sup>SKY</sup>-LIVER<sup>Hu</sup> 2.0, A Publicly Available Database* (SSRN Scholarly Paper 3905926). <https://doi.org/10.2139/ssrn.3905926>

Li, H., Zhang, H., Huang, G., Bing, Z., Xu, D., Liu, J., Luo, H., & An, X. (2022). Loss of RPS27a expression regulates the cell cycle, apoptosis, and proliferation via the RPL11-MDM2-p53 pathway in lung adenocarcinoma cells. *Journal of Experimental & Clinical Cancer Research*, 41(1), 33. <https://doi.org/10.1186/s13046-021-02230-z>

Liang, C., Shi, S., Qin, Y., Meng, Q., Hua, J., Hu, Q., Ji, S., Zhang, B., Xu, J., & Yu, X.-J. (2020). Localisation of PGK1 determines metabolic phenotype to balance metastasis and proliferation in patients with SMAD4-negative pancreatic cancer. *Gut*, 69(5), 888–900. <https://doi.org/10.1136/gutjnl-2018-317163>

Lin, C.-Y., Lin, L.-Y., Wen, T.-W., Lien, G.-W., Chien, K.-L., Hsu, S. H. J., Liao, C.-C., Sung, F.-C., Chen, P.-C., & Su, T.-C. (2013). Association between levels of serum perfluorooctane sulfate and carotid artery intima-media thickness in adolescents and young adults. *International Journal of Cardiology*, 168(4), 3309–3316. <https://doi.org/10.1016/j.ijcard.2013.04.042>

Liu, B., Zhang, R., Zhang, H., Yu, Y., Yao, D., & Yin, S. (2020). Levels of Perfluoroalkyl Acids (PFAAs) in Human Serum, Hair and Nails in Guangdong Province, China: Implications for Exploring the Ideal Bio-Indicator. *Archives of Environmental Contamination and Toxicology*, 79(2), 184–194. <https://doi.org/10.1007/s00244-020-00743-w>

Liu, J., Du, X., Zhou, J., Pan, Z., Liu, H., & Li, Q. (2014). MicroRNA-26b Functions as a Proapoptotic Factor in Porcine Follicular Granulosa Cells by Targeting Sma- and Mad-Related

Protein 41. *Biology of Reproduction*, 91(6), 146, 1–12. <https://doi.org/10.1095/biolreprod.114.122788>

Mah, L.-J., El-Osta, A., & Karagiannis, T. C. (2010).  $\gamma$ H2AX: A sensitive molecular marker of DNA damage and repair. *Leukemia*, 24(4), Article 4. <https://doi.org/10.1038/leu.2010.6>

Maréchal, A., & Zou, L. (2013). DNA Damage Sensing by the ATM and ATR Kinases. *Cold Spring Harbor Perspectives in Biology*, 5(9), a012716. <https://doi.org/10.1101/cshperspect.a012716>

Masereeuw, R. (2022). The Dual Roles of Protein-Bound Solutes as Toxins and Signaling Molecules in Uremia. *Toxins*, 14(6), Article 6. <https://doi.org/10.3390/toxins14060402>

Moein, S., Javanmard, S. H., Abedi, M., Izadpanahi, M. H., & Gheisari, Y. (2017). Identification of Appropriate Housekeeping Genes for Gene Expression Analysis in Long-term Hypoxia-treated Kidney Cells. *Advanced Biomedical Research*, 6(1), 15. <https://doi.org/10.4103/2277-9175.200790>

Papageorgis, P., Cheng, K., Ozturk, S., Gong, Y., Lambert, A. W., Abdolmaleky, H. M., Zhou, J.-R., & Thiagalingam, S. (2011). Smad4 Inactivation Promotes Malignancy and Drug Resistance of Colon Cancer. *Cancer Research*, 71(3), 998–1008. <https://doi.org/10.1158/0008-5472.CAN-09-3269>

Pierozaan, P., Cattani, D., & Karlsson, O. (2020). Perfluorooctane sulfonate (PFOS) and perfluorooctanoic acid (PFOA) induce epigenetic alterations and promote human breast cell carcinogenesis in vitro. *Archives of Toxicology*, 94(11), 3893–3906. <https://doi.org/10.1007/s00204-020-02848-6>

Poothong, S., Papadopoulou, E., Padilla-Sánchez, J. A., Thomsen, C., & Haug, L. S. (2020). Multiple pathways of human exposure to poly- and perfluoroalkyl substances (PFASs): From external exposure to human blood. *Environment International*, 134, 105244. <https://doi.org/10.1016/j.envint.2019.105244>

Schwen, L. O., Schenk, A., Kreutz, C., Timmer, J., Rodríguez, M. M. B., Kuepfer, L., & Preusser, T. (2015). Representative Sinusoids for Hepatic Four-Scale Pharmacokinetics Simulations. *PLOS ONE*, 10(7), e0133653. <https://doi.org/10.1371/journal.pone.0133653>

Shearer, J. J., Callahan, C. L., Calafat, A. M., Huang, W.-Y., Jones, R. R., Sabbiseti, V. S., Freedman, N. D., Sampson, J. N., Silverman, D. T., Purdue, M. P., & Hofmann, J. N. (2021). Serum Concentrations of Per- and Polyfluoroalkyl Substances and Risk of Renal Cell Carcinoma. *JNCI: Journal of the National Cancer Institute*, 113(5), 580–587. <https://doi.org/10.1093/jnci/djaa143>

Son, H.-Y., Kim, S.-H., Shin, H.-I., Bae, H. I., & Yang, J.-H. (2008). Perfluorooctanoic acid-induced hepatic toxicity following 21-day oral exposure in mice. *Archives of Toxicology*, 82(4), 239–246. <https://doi.org/10.1007/s00204-007-0246-x>

Suberbielle, E., Sanchez, P. E., Kravitz, A. V., Wang, X., Ho, K., Eilertson, K., Devidze, N., Kreitzer, A. C., & Mucke, L. (2013). Physiologic brain activity causes DNA double-strand breaks in neurons, with exacerbation by amyloid- $\beta$ . *Nature Neuroscience*, *16*(5), Article 5. <https://doi.org/10.1038/nn.3356>

Sun, S., Guo, H., Wang, J., & Dai, J. (2019). Hepatotoxicity of perfluorooctanoic acid and two emerging alternatives based on a 3D spheroid model. *Environmental Pollution*, *246*, 955–962. <https://doi.org/10.1016/j.envpol.2018.12.065>

Sunderland, E. M., Hu, X. C., Dassuncao, C., Tokranov, A. K., Wagner, C. C., & Allen, J. G. (2019). A review of the pathways of human exposure to poly- and perfluoroalkyl substances (PFASs) and present understanding of health effects. *Journal of Exposure Science & Environmental Epidemiology*, *29*(2), Article 2. <https://doi.org/10.1038/s41370-018-0094-1>

Ubel, F. A., Sorenson, S. D., & Roach, D. E. (1980). Health status of plant workers exposed to fluorochemicals—A preliminary report. *American Industrial Hygiene Association Journal*, *41*(8), 584–589. <https://doi.org/10.1080/15298668091425310>

Vieira, V. M., Hoffman, K., Shin, H.-M., Weinberg, J. M., Webster, T. F., & Fletcher, T. (2013). Perfluorooctanoic Acid Exposure and Cancer Outcomes in a Contaminated Community: A Geographic Analysis. *Environmental Health Perspectives*, *121*(3), 318–323. <https://doi.org/10.1289/ehp.1205829>

Voorneveld, P. W., Kodach, L. L., Jacobs, R. J., Liv, N., Zonneville, A. C., Hoogenboom, J. P., Biemond, I., Verspaget, H. W., Hommes, D. W., Rooij, K. de, Noesel, C. J. M. van, Morreau, H., Wezel, T. van, Offerhaus, G. J. A., Brink, G. R. van den, Peppelenbosch, M. P., Dijke, P. ten, & Hardwick, J. C. H. (2014). Loss of SMAD4 Alters BMP Signaling to Promote Colorectal Cancer Cell Metastasis via Activation of Rho and ROCK. *Gastroenterology*, *147*(1), 196-208.e13. <https://doi.org/10.1053/j.gastro.2014.03.052>

Wang, Y., Zhong, Y., Li, J., Zhang, J., Lyu, B., Zhao, Y., & Wu, Y. (2018). Occurrence of perfluoroalkyl substances in matched human serum, urine, hair and nail. *Journal of Environmental Sciences (China)*, *67*, 191–197. <https://doi.org/10.1016/j.jes.2017.08.017>

Wen, Y., Mirji, N., & Irudayaraj, J. (2020). Epigenetic toxicity of PFOA and GenX in HepG2 cells and their role in lipid metabolism. *Toxicology in Vitro*, *65*, 104797. <https://doi.org/10.1016/j.tiv.2020.104797>

Yan, C., Yang, Q., Shen, H.-M., Spitsbergen, J. M., & Gong, Z. (2017). Chronically high level of tgfb1a induction causes both hepatocellular carcinoma and cholangiocarcinoma via a dominant Erk pathway in zebrafish. *Oncotarget*, *8*(44), 77096–77109. <https://doi.org/10.18632/oncotarget.20357>

Yan, P., Klingbiel, D., Saridaki, Z., Ceppa, P., Curto, M., McKee, T. A., Roth, A., Tejpar, S., Delorenzi, M., Bosman, F. T., & Fiocca, R. (2016). Reduced Expression of SMAD4 Is Associated

with Poor Survival in Colon Cancer. *Clinical Cancer Research*, 22(12), 3037–3047. <https://doi.org/10.1158/1078-0432.CCR-15-0939>

Yao, X., & Zhong, L. (2005). Genotoxic risk and oxidative DNA damage in HepG2 cells exposed to perfluorooctanoic acid. *Mutation Research/Genetic Toxicology and Environmental Mutagenesis*, 587(1), 38–44. <https://doi.org/10.1016/j.mrgentox.2005.07.010>

Zane, L., & Schultz, T. (2020). Cytotoxicity of Environmental Toxins PFOA and Gen X. *Ocean Sciences Meeting 2020*.

Zhang, S., Chen, K., Li, W., Chai, Y., Zhu, J., Chu, B., Li, N., Yan, J., Zhang, S., & Yang, Y. (2021). Varied thyroid disrupting effects of perfluorooctanoic acid (PFOA) and its novel alternatives hexafluoropropylene-oxide-dimer-acid (GenX) and ammonium 4,8-dioxa-3H-perfluorononanoate (ADONA) in vitro. *Environment International*, 156, 106745. <https://doi.org/10.1016/j.envint.2021.106745>

Zhao, M., Mishra, L., & Deng, C.-X. (2018). The role of TGF- $\beta$ /SMAD4 signaling in cancer. *International Journal of Biological Sciences*, 14(2), 111–123. <https://doi.org/10.7150/ijbs.23230>